Article

Cell Reports

Plk1/Polo Phosphorylates Sas-4 at the Onset of Mitosis for an Efficient Recruitment of Pericentriolar Material to Centrosomes

Graphical Abstract

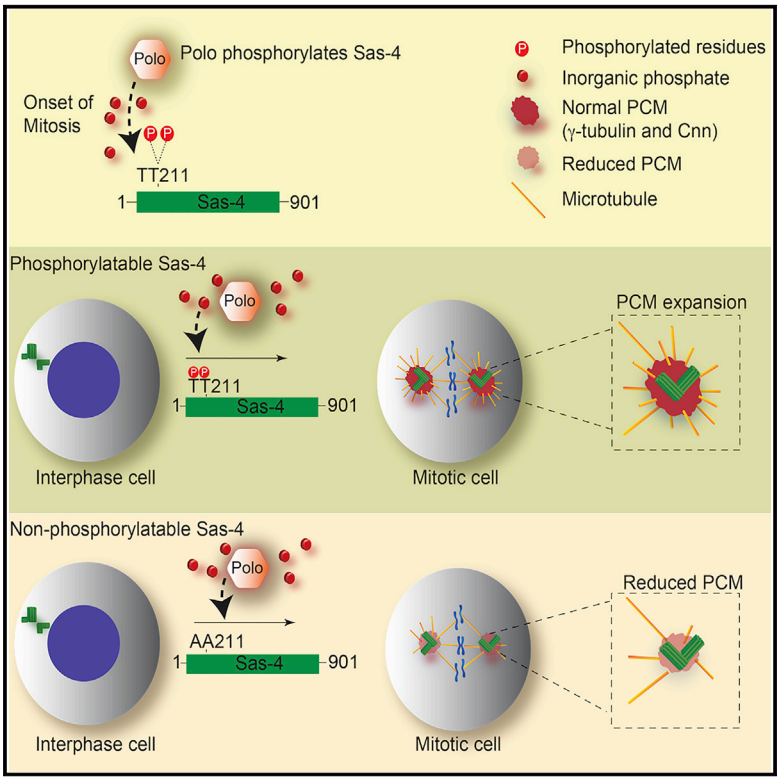

Highlights

- *Drosophila* Sas-4 is phosphorylated by Plk1/Polo at the onset of mitosis
- Cell-cycle-specific Sas-4 antibodies identify spatiotemporal dynamics of Sas-4
- Sas-4 phosphorylation at TT211 site is required for recruitment of Cnn and γ-tubulin
- Phosphorylation status of Sas-4 determines the PCM size of mitotic centrosomes

Authors

Anand Ramani, Aruljothi Mariappan, Marco Gottardo, ..., Alain Debec, Regina Feederle, Jay Gopalakrishnan

Correspondence

jay.gopalakrishnan@hhu.de

In Brief

Ramani et al. show that Plk1/Polo phosphorylates *Drosophila* Sas-4 at the onset of mitosis. Cell-cycle-specific modification of Sas-4 determines the spatiotemporal localization of Sas-4 in centrosomes, which is required for an efficient recruitment of PCM proteins in mitosis.

Ramani et al., 2018, Cell Reports *25*, 3618–3630
December 26, 2018
https://doi.org/10.1016/j.celrep.2018.11.102

CellPress

OPEN ACCESS
CellPress

Cell Reports
Article

Plk1/Polo Phosphorylates Sas-4 at the Onset of Mitosis for an Efficient Recruitment of Pericentriolar Material to Centrosomes

Anand Ramani,[1,2,3] Aruljothi Mariappan,[1,2] Marco Gottardo,[1,2] Sunit Mandad,[4,5,6] Henning Urlaub,[4,5] Tomer Avidor-Reiss,[7] Maria Riparbelli,[8] Giuliano Callaini,[8] Alain Debec,[9] Regina Feederle,[10] and Jay Gopalakrishnan[1,2,3,11,*]

[1]Institute of Human Genetics, Universitätsklinikum Heinrich-Heine-Universität Düsseldorf, Universität Str. 1, 40225 Düsseldorf, Germany
[2]Center for Molecular Medicine Cologne, University of Cologne, Robert-Koch-Str. 21, 50931 Cologne, Germany
[3]IUF–Leibniz-Institut für umweltmedizinische Forschung gGmbH, Auf'm Hennekamp 50, 40225 Düsseldorf, Germany
[4]Bioanalytical Mass Spectrometry Group, Max Planck Institute for Biophysical Chemistry, Am Fassberg 11, 37077 Göttingen, Germany
[5]Bioanalytics, University Medical Center Goettingen, Robert-Koch-Strasse 40, 37075 Goettingen, Germany
[6]Department of Neuro- and Sensory Physiology, University Medical Center Göttingen, Göttingen, Germany
[7]Department of Biological Sciences, College of Natural Sciences and Mathematics, University of Toledo, Toledo, OH 43606
[8]Department of Life Sciences, University of Siena, 53100 Siena, Italy
[9]Polarity and Morphogenesis Group, Institut Jacques Monod, Centre National de la Recherche Scientifique, University Paris Diderot, 75013 Paris, France
[10]Helmholtz Zentrum München, German Research Center for Environmental Health, Institute for Diabetes and Obesity, Core Facility, 81377 Munich, Germany
[11]Lead Contact
*Correspondence: jay.gopalakrishnan@hhu.de
https://doi.org/10.1016/j.celrep.2018.11.102

SUMMARY

Centrosomes are the major microtubule-organizing centers, consisting of centrioles surrounded by a pericentriolar material (PCM). Centrosomal PCM is spatiotemporally regulated to be minimal during interphase and expands as cells enter mitosis. It is unclear how PCM expansion is initiated at the onset of mitosis. Here, we identify that, in *Drosophila*, Plk1/Polo kinase phosphorylates the conserved centrosomal protein Sas-4 *in vitro*. This phosphorylation appears to occur at the onset of mitosis, enabling Sas-4's localization to expand outward from meiotic and mitotic centrosomes. The Plk1/Polo kinase site of Sas-4 is then required for an efficient recruitment of Cnn and γ-tubulin, bona fide PCM proteins that are essential for PCM expansion and centrosome maturation. Point mutations at Plk1/Polo sites of Sas-4 affect neither centrosome structure nor centriole duplication but specifically reduce the affinity to bind Cnn and γ-tubulin. These observations identify Plk1/Polo kinase regulation of Sas-4 as essential for efficient PCM expansion.

INTRODUCTION

Centrosomes have many important cellular functions. Among them is serving as the major microtubule-organizing center (MTOC) in regulating the organization of bipolar spindles for accurate cell division (Conduit and Raff, 2015; Tang and Marshall, 2012). At their core, centrosomes are composed of a pair of centrioles surrounded by pericentriolar material (PCM) formed by various multiprotein complexes (Avidor-Reiss and Gopalakrishnan, 2013; Nigg, 2004; Nigg and Raff, 2009) (Conduit et al., 2014) (Nigg and Holland, 2018). During cell division, centrosomes undergo a strict duplication cycle so that each daughter cell receives a centrosome. At interphase of the cell cycle, when centrioles duplicate, the centrosome contains a basal level of PCM and is incompetent to nucleate robust microtubules. However, as cells enter into mitosis, duplicated centrosomes recruit PCM and expand in size (Conduit et al., 2010; Gopalakrishnan et al., 2012). The process of PCM recruitment enabling centrosomes to be functional organelles in mitosis is called centrosome maturation. Centrosome maturation is not only essential for MTOC function of centrosomes but also critical for newborn daughter centriole-to-centrosome conversion (Fu et al., 2016; Novak et al., 2016).

Mechanisms of PCM recruitment have been studied in various organisms. As an example, in fly embryos, Spd-2 recruits Cnn, a bona fide PCM protein, which is phosphorylated by Polo kinase and is required for expanding PCM during mitosis (Conduit and Raff, 2010; Dix and Raff, 2007; Giansanti et al., 2008). Likewise, in worms, spindle-defective protein 5 (SPD-5), a distant ortholog of Cnn, is recruited to centrioles in an SPD-2-dependent manner, which is then phosphorylated by Plk1/Polo kinase, allowing SPD-5 to assemble mitotic centrosomes (Woodruff et al., 2015; Wueseke et al., 2016). Cnn recruitment in flies also seems to be initiated by Asterless (Asl), another centrosomal protein that functions at early stages of centrosome duplication (Blachon et al., 2008; Novak et al., 2014). Recently, it has been shown that Asl recruitment to the daughter centrioles of fly embryos is

directly dependent on the Cdk1-mediated phosphorylation status of the conserved centrosomal protein Sas-4 (Novak et al., 2016).

Earlier studies revealed that Plk1/Polo kinase, Cnn, and Asl interact with Sas-4 (Conduit et al., 2015; Gopalakrishnan et al., 2011). Thus, it appears that during PCM recruitment to a centrosome, Sas-4 functions upstream to Asl and Cnn. First, because Sas-4 provides a scaffold for S-CAP complexes (Sas-4 and components of PCM proteins such as Cnn, Asl, and PLP) (Conduit et al., 2015; Gopalakrishnan et al., 2011) and second, Sas-4 closely associates with the centriolar wall, providing an interface to mediate PCM tethering to the centriole (Fu and Glover, 2012; Gopalakrishnan et al., 2011; Zheng et al., 2014). However, how the timing and amount of PCM recruitment is determined has yet to be critically analyzed.

Our biochemical studies have identified that tubulin negatively affects Sas-4's ability to form cytoplasmic protein complexes (Gopalakrishnan et al., 2011, 2012; Zheng et al., 2016). *Drosophila* expressing a Sas-4 variant that does not bind tubulin exhibited abnormal PCM recruitment. In this mutant fly, the major PCM protein Cnn, normally abundant in mitotic centrosomes, was observed in interphase centrosomes, while mitotic centrosomes recruited at least twice the amount of Cnn as control centrosomes (Gopalakrishnan et al., 2012). These results suggested that tubulin present in wild-type Sas-4 complexes spatiotemporally regulates the amount of PCM recruitment (i.e., tubulin can function as a molecular switch in regulating Sas-4-mediated PCM recruitment). While these studies have substantiated the S-CAP complexes as components of PCM, at what stage of the cell cycle the S-CAP components are sequentially recruited to distinct domains of the centrosome has remained unclear.

With an application of advanced light microscopy techniques, a recent study using fluorescently tagged centrosomal proteins has elegantly shown distinct patterns of Sas-4, Asl, and Cnn recruitment to interphase centrioles (Conduit et al., 2015). The localization patterns of these proteins in a centrosome reaffirm the findings by the original super-resolution studies that imaged native centrosomal proteins in *Drosophila* and human centrosomes (Fu and Glover, 2012; Mennella et al., 2014) (Lawo et al., 2012). Although these studies provide greater insights into PCM recruitment, the crucial steps that initiate PCM growth, in particular, the upstream events that prime PCM recruitment to centrosomes at the onset of mitosis, remain unclear.

Here, by generating cell-cycle-specific Sas-4 antibodies, we identify that in *Drosophila*, Sas-4 can be phosphorylated by Plk1/Polo kinase. This phosphorylation appears to occur at the onset of mitosis, enabling Sas-4 to expand its localization, growing outward from meiotic and mitotic centrosomes. The Sas-4 residues that can be phosphorylated by Plk1/Polo are then required for an efficient recruitment of Cnn and γ-tubulin for PCM expansion during cell division. Cnn and γ-tubulin recruitments were independent from Asl recruitment. Thus, Plk1/Polo kinase regulation of Sas-4 appears to be a critical step at the early events of PCM expansion in building meiotic and mitotic centrosomes.

RESULTS

Sas-4 Is Post-translationally Modified at the Onset of Mitosis

To identify potential cell-cycle-dependent post-translational modification sites in Sas-4, we took an antibody-based approach using our mouse monoclonal antibodies generated against amino acids 1–350 of Sas-4 (Figure 1A). One of the clones (hereafter anti-Sas-4) recognized Sas-4 at centrosomes of *Drosophila* cells (Schneider cells) throughout the cell cycle (Figure 1B, i). The epitope-containing region for this antibody is present within the PN2-3 domain at the N terminus of Sas-4 (Figure 1A) (Gopalakrishnan et al., 2011, 2012; Hung et al., 2004). Another clone for which the epitope-containing region is 190-LIGKNACSSTPDLKS SYASSTTASSTSPRV-220 recognized Sas-4 at both centrosomal pairs of the interphase and prophase, similar to anti-Sas-4. However, using this antibody, we could not detect Sas-4 in either of the centrosomes of mitosis (hereafter non-mitotic anti-Sas-4) (Figure 1B, ii).

To investigate the localization pattern of Sas-4 recognized by the non-mitotic anti-Sas-4 at subdiffraction resolution, we performed stimulated emission depletion (STED) microscopy with ~50 nm lateral, 120 nm axial resolution (Fu et al., 2016). It is known that Sas-4 preferentially localizes to the daughter centrioles, which in turn then recruits another centrosomal protein Asl (Novak et al., 2014, 2016). Asl is recruited to daughter centrioles only after the centrosomes are disengaged at the end of mitosis (Novak et al., 2014). Thus, in our analysis, we used Asl labeling to distinguish mother centrioles from daughter centrioles. Notably, the non-mitotic anti-Sas-4 preferentially recognized Sas-4 at daughter centrioles at interphase and prophase (Figure 1C, i and ii). Even at this subdiffraction resolution, we could not detect Sas-4 in either of the metaphase centrosomes (Figure 1C, iii). This finding suggests that the epitope for non-mitotic anti-Sas-4 appears to be post-translationally modified at the onset of metaphase.

Sas-4-TT211 Can Be Phosphorylated at the Onset of Mitosis

We then aimed to identify whether there are phosphorylatable residues within the epitope-containing region (190-LIGK NACSSTPDLKSSYASSTTASSTSPRV-220) of the non-mitotic anti-Sas-4 antibody. We noticed that there are at least two regions, namely -P1 and -P2 sites, containing threonine and serine residues that can be phosphorylated (Figure 2A). To identify the responsible residues for the non-mitotic anti-Sas-4, we expressed recombinant Sas-4 proteins (amino acids 1–350) containing deletions or replacements and probed them using the non-mitotic anti-Sas-4 (Figures S1A and S1B). This antibody failed to recognize the protein in which both -P1 and -P2 sites were deleted (Figure S1C). However, this antibody recognized the replacement of the -P1 but not the -P2 site, suggesting that the -P2 site harboring -SSTT211 (we number the first threonine) is a responsible residue for the non-mitotic anti-Sas-4. It has been recently shown that Cdk1 phosphorylates Sas-4's threonine at 200 (Sas-4-T200) of the -P1 site at the onset of mitosis (Novak et al., 2016).

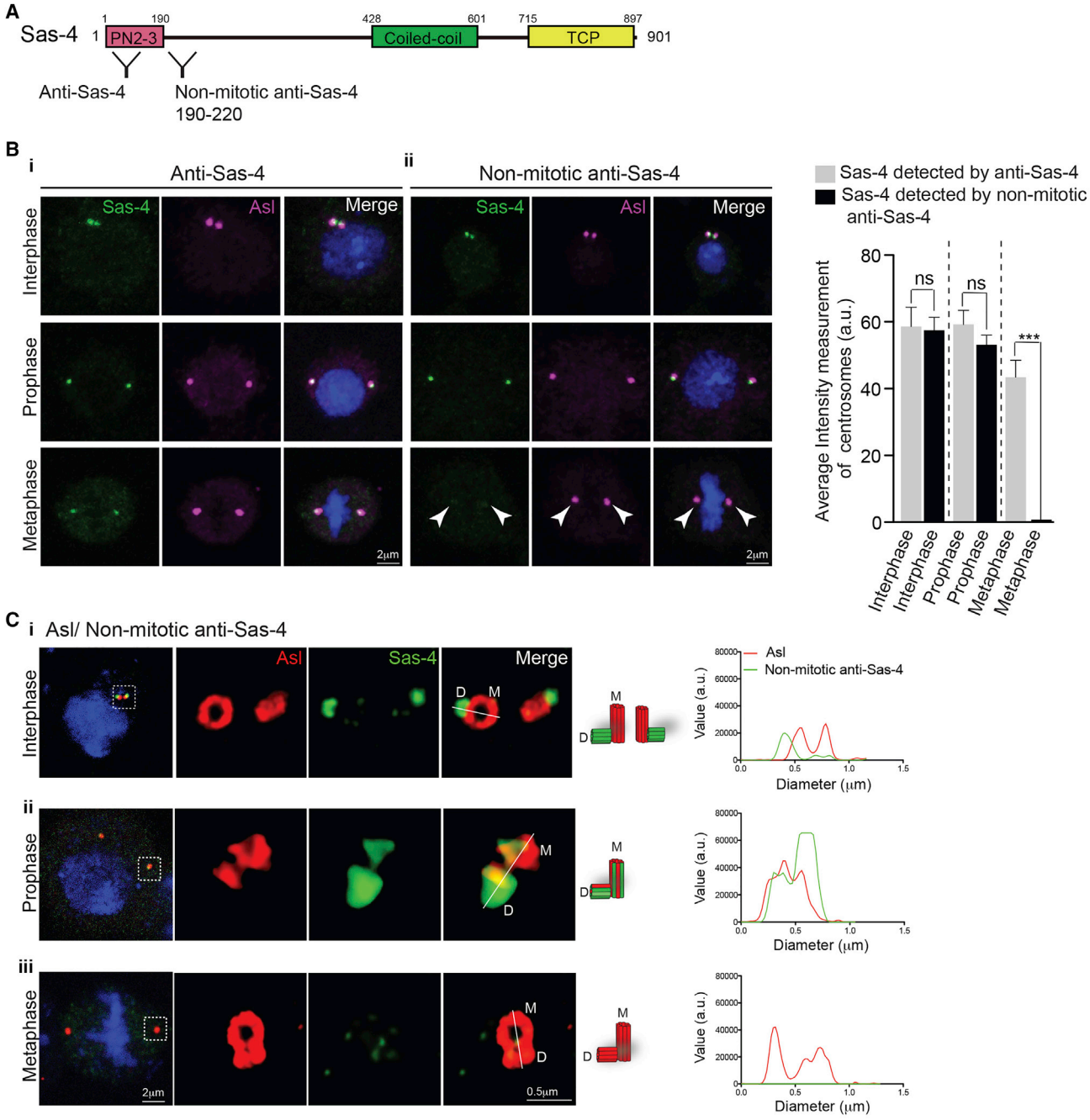

Figure 1. Non-mitotic Anti-Sas-4 Recognizes Centrosomal Sas-4 from Interphase through Prophase but Not at Metaphase

(A) Schematic of Sas-4 protein indicating epitope regions for anti-Sas-4 and non-mitotic anti-Sas-4 antibodies.

(B) Anti-Sas-4 antibody (green) recognizes Sas-4 at centrosomes of *Drosophila* cells (Schneider cells) throughout the cell cycle. Asl (magenta) labels centrosomes (i). In contrast, non-mitotic anti-Sas-4 does not recognize metaphase Sas-4 (arrowheads) (ii). Bar graph at right represents the average intensity measurements of centrosomes (labeled by anti-Sas-4 and non-mitotic anti-Sas-4). At least 60 centrosomes (n = 60) were analyzed from 3 independent experiments. ANOVA, ***$p < 0.0001$. Error bars represent means ± SEMs. See also Figure S1.

(C) Characterization of non-mitotic anti-Sas-4 using stimulated emission depletion (STED) microscopy. At interphase (before centrosomes disengage), non-mitotic anti-Sas-4 preferentially recognizes Sas-4 at the daughter centrioles (green). Note that Asl (red) labels only mother centrioles at interphase (i). At prophase (after centrosomes disengage), non-mitotic anti-Sas-4 also recognizes mother centrioles. Note that Asl starts to label daughter centrioles where Sas-4 is abundant (ii). At metaphase, non-mitotic anti-Sas-4 recognizes neither of the centrioles. At this stage, Asl (red) labels both mother and daughter centrioles. Illustrations of centrioles containing Asl and Sas-4 are at right. Line graph representing the relative distribution of proteins at the mother and daughter centrioles of various cell-cycle stages is at right. At least 30 mitotic centrosomes (n = 30) were analyzed for each antibody.

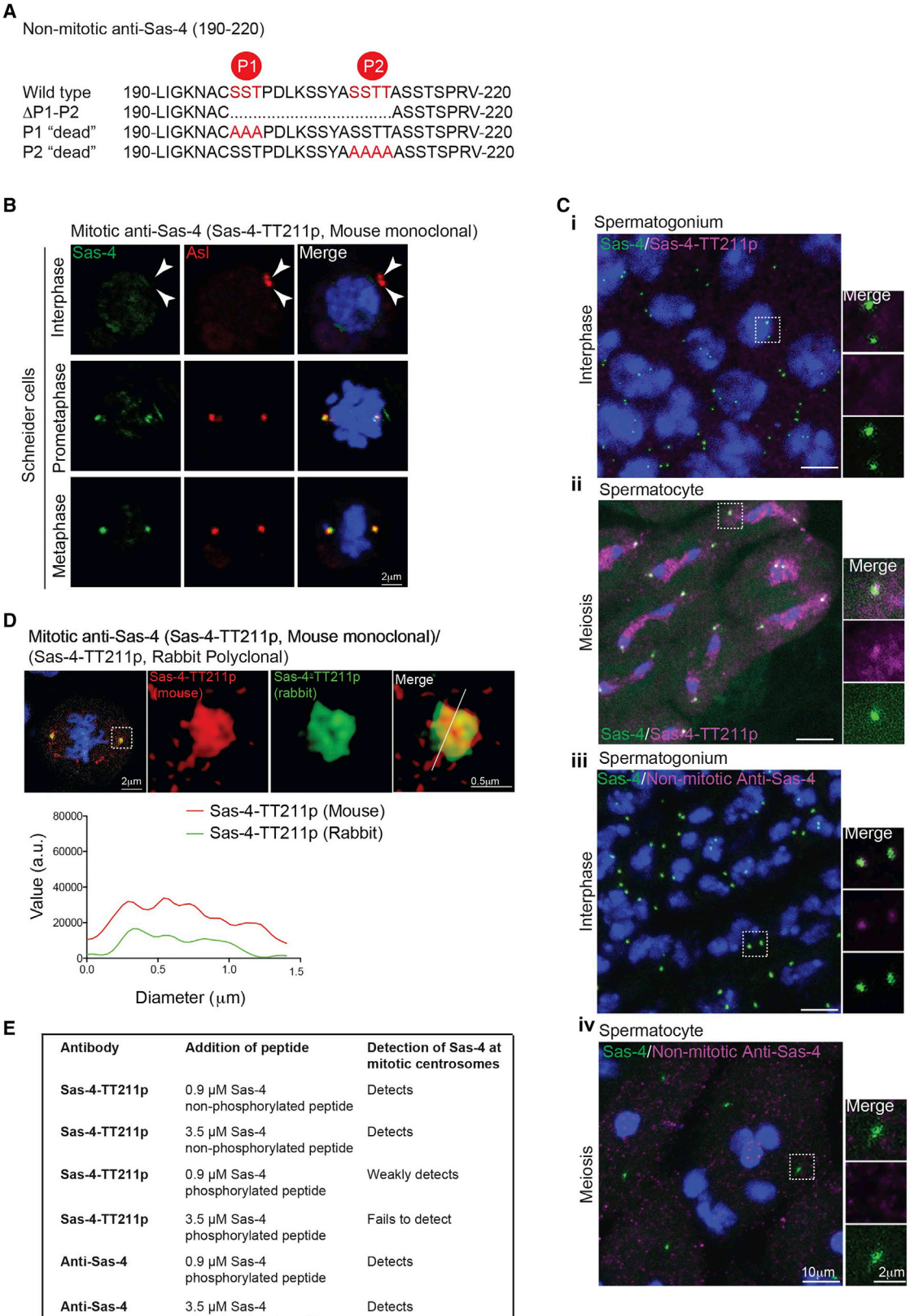

E

Antibody	Addition of peptide	Detection of Sas-4 at mitotic centrosomes
Sas-4-TT211p	0.9 μM Sas-4 non-phosphorylated peptide	Detects
Sas-4-TT211p	3.5 μM Sas-4 non-phosphorylated peptide	Detects
Sas-4-TT211p	0.9 μM Sas-4 phosphorylated peptide	Weakly detects
Sas-4-TT211p	3.5 μM Sas-4 phosphorylated peptide	Fails to detect
Anti-Sas-4	0.9 μM Sas-4 phosphorylated peptide	Detects
Anti-Sas-4	3.5 μM Sas-4 phosphorylated peptide	Detects

(legend on next page)

To further narrow down the epitope residues, we generated peptides with single amino acid replacements within the -P2 site (-SSTT211) and performed dot blots. The non-mitotic anti-Sas-4 recognized all of the single amino acid replacements with alanine (Figure S1D). However, replacing double amino acids with two-alanine -SSTT211 to -SSAA211 narrowed down the responsible residues for the non-mitotic anti-Sas-4 to be -TT211 (Figure S1E).

We then generated mouse monoclonal and rabbit polyclonal antibodies using a peptide (207-YASS**TT**ASSTSPRV-220) as an antigen in which both of the threonine -TT211s are phosphorylated. The resulting antibodies are called mitotic anti-Sas-4 (Sas-4-TT211p, where TTp denotes phosphorylated threonine residues). These antibodies specifically recognize a peptide that harbors two-phosphorylated threonine at -TT211 (Figure S1F). Although the mitotic anti-Sas-4 (Sas-4-TT211p) did not satisfactorily detect the protein in the western blots, both of these antibodies recognized Sas-4 not at the interphase but starting from prometaphase, suggesting that -TT211s are phosphorylated at the onset of mitosis (Figure 2B). Similarly, these antibodies did recognize only dividing sperm cells in *Drosophila* testes (Figure 2C). The labeling patterns of both of these antibodies at mitotic centrosomes were nearly identical, as demonstrated by STED microscopy (Figure 2D).

To validate the specificity of Sas-4-TT211p antibodies, we used Schneider cells (C131), which lack endogenous Sas-4 and centrosomes. Sas-4-TT211p antibodies could recognize centrosomes only when these cells were transfected with the Sas-4-GFP construct (Figure S1G). To further test whether Sas-4-TT211 is phosphorylated in cells, we performed a competition experiment with increasing concentrations of phosphorylated peptide (207-YASS**TT**ASSTSPRV-220), which could hinder the Sas-4-TT211p antibody from binding to the phosphorylated version of endogenous Sas-4 (Figure S2). In control experiments, we used a non-phosphorylated peptide (207-YASSTTASS TSPRV-220). At 0.9 μM phosphorylated peptide, the antibody could faintly recognize Sas-4 at mitotic centrosomes. However, at 3.5 μM phosphorylated peptide, the antibody nearly failed to recognize Sas-4 at mitotic centrosomes (Figures S2A and S2B). In contrast, in the presence of the non-phosphorylated peptide (both at 0.9 and 3.5 μM), Sas-4-TT211p could recognize Sas-4 normally at mitotic centrosomes (Figures S2C and S2D). Neither of these peptides prevented anti-Sas-4 (which labels Sas-4 throughout the cell cycle) from recognizing Sas-4 at mitotic centrosomes (Figures S2E and S2F). The schematic of this experiment and the results are summarized in Figures S2G and 2E. It is noteworthy that centrosome maturation begins with PCM recruitment, which occurs at the onset of mitosis.

In summary, we have obtained three different anti-Sas-4 antibodies, namely (1) anti-Sas-4, which recognizes centrosomal Sas-4 throughout the cell-cycle phases (Figure 1Bi); (2) non-mitotic anti-Sas-4, which recognizes Sas-4 only up to the prophase-like stage (Figures 1B, ii, and 1C); and (3) mitotic anti-Sas-4 (Sas-4-TT211p), which recognizes Sas-4 only at the onset of mitosis (Figures 2B, 2C, and S1H).

Plk1/Polo Can Phosphorylate Sas-4-TT211 *In Vitro*

At interphase, Sas-4 is incorporated into newly forming centrioles (Dammermann et al., 2008) (Figure 1C). In mitotic centrosomes where no centriole duplication occurs, Sas-4 is stably incorporated within mother centrioles, and no new Sas-4 is synthesized or exchanged from the cytoplasmic pool (Dammermann et al., 2008; Novak et al., 2014). This finding has possibly precluded the idea of Sas-4 being involved in mitotic PCM recruitment. However, a recent work showed that Cdk1 phosphorylates Sas-4's T200 at the onset of mitosis, providing a Polo docking site, which in turn recruits the PCM protein Asl to daughter centrioles of mitotic centrosomes (Novak et al., 2016). In addition, it is known that Plk1/Polo is required for the dramatic increase in PCM that occurs before mitotic entry in Schneider cells (Riparbelli et al., 2014; Asteriti et al., 2015; Haren et al., 2009). From these, we hypothesized that Plk1/Polo docking could phosphorylate Sas-4, which triggers the further recruitment of PCM components such as Cnn and γ-tubulin, which determine centrosome size.

It is known that Plk1/Polo kinase co-immunoprecipitates with Sas-4 (Gopalakrishnan et al., 2011) (Figure 3A). To determine whether Plk1/Polo can phosphorylate Sas-4's TT211, we tested whether Plk1/Polo kinase can directly interact with Sas-4. We found that wild-type recombinant Sas-4 1–350 could bind recombinant Plk1/Polo kinase. Deleting both -P1 and -P2 sites significantly reduced the binding capacity of Sas-4 to Plk1/Polo kinase (Figure 3B). To analyze whether Plk1/Polo kinase can specifically phosphorylate Sas-4-TT211, we extended our *in vitro* kinase assay on a Sas-4 peptide (207-YASSTTA SSTSPRV-220) that contained the epitope region for the non-mitotic anti-Sas-4 (Figure 3C). We took this peptide-based approach to avoid non-specific phosphorylation in sites other than the epitope-containing region. In positive controls, we used a Sas-4 phosphopeptide in which -TT211s are phosphorylated. In negative controls, we used an Sas-4 mutant peptide in which two of the threonines is replaced with non-phosphorylatable

Figure 2. Sas-4-TT211 Is Phosphorylated at the Onset of Mitosis

(A) Epitope-containing region (190-LIGKNACSSTPDLKSSYASSTTASSTSPRV-220) of the non-mitotic anti-Sas-4 displaying -P1 and -P2 sites (red). Different peptides used in this study are given.

(B) Mitotic anti-Sas-4 (Sas-4-TT211p) specifically recognizes centrosomal Sas-4 at prometaphase and metaphase (green). Note that mitotic anti-Sas-4 (Sas-4-TT211p) does not recognize interphase centrosomes (arrowheads). Asl (red) labels centrosomes. At least 60 mitotic centrosomes (n = 60) were analyzed for each condition. See also Figures S1 and S2.

(C) Sas-4-TT211p (i and ii, magenta) specifically labels mitotic centrosomes of *Drosophila* spermatocytes expressing Sas-4-GFP (green). The non-mitotic anti-Sas-4 (iii and iv, magenta) fails to recognize mitotic centrosomes, but specifically recognizes interphase centrosomes expressing Sas-4-GFP (green). At least 40 mitotic centrosomes (n = 40) were analyzed for each condition.

(D) STED imaging of mitotic centrosomes labeled by both mouse monoclonal and rabbit polyclonal mitotic anti-Sas-4 (Sas-4-TT211p). Line graphs representing the relative distributions of Sas-4 recognized by these antibodies are provided below. At least 20 mitotic centrosomes (n = 20) were analyzed for each condition.

(E) The table provides a summary of the Sas-4 peptide-based competition experiment in Schneider cells to confirm the specificity of Sas-4-TT211p antibody.

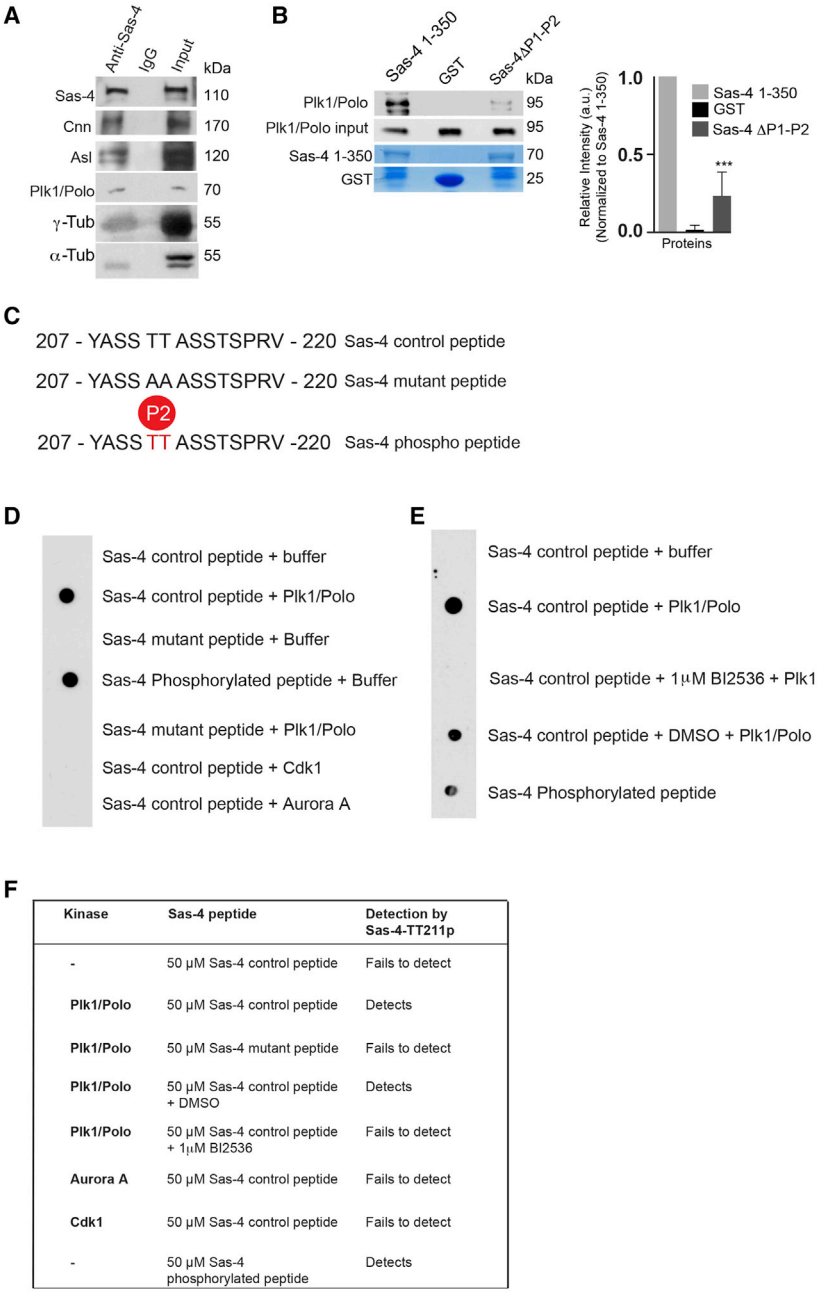

F

Kinase	Sas-4 peptide	Detection by Sas-4-TT211p
-	50 μM Sas-4 control peptide	Fails to detect
Plk1/Polo	50 μM Sas-4 control peptide	Detects
Plk1/Polo	50 μM Sas-4 mutant peptide	Fails to detect
Plk1/Polo	50 μM Sas-4 control peptide + DMSO	Detects
Plk1/Polo	50 μM Sas-4 control peptide + 1μM BI2536	Fails to detect
Aurora A	50 μM Sas-4 control peptide	Fails to detect
Cdk1	50 μM Sas-4 control peptide	Fails to detect
-	50 μM Sas-4 phosphorylated peptide	Detects

Figure 3. Plk1/Polo Can Bind and Phosphorylate Sas-4-TT211 *In Vitro*

(A) Immunopurification of Sas-4 complexes from *Drosophila* embryonic extracts using the anti-Sas-4 antibody. Plk1/Polo along with the S-CAP components co-immunoprecipitate with Sas-4. Immunoglobulin G (IgG)-coated beads are used as the control.

(B) Plk1/Polo directly interacts with Sas-4 1–350. Note that the deletion version of Sas-4 1-350 (190-LIGKNACSSTPDLKSSYASSTTASSTSPRV-220), in which the epitope region for the non-mitotic and mitotic anti-Sas-4 antibodies are eliminated, exhibits a reduced binding capacity. Coomassie blue staining of recombinant Sas-4 1–350 is given at bottom. The bar graph at right represents the relative intensity of Plk1/Polo interaction with Sas-4 variants. ANOVA, ***$p < 0.0001$. Error bars represent means ± SEMs from 3 independent experiments. See also Figure S3.

(C) Various peptides spanning the epitope for the mitotic anti-Sas-4 antibody (Sas-4-TT211p). Note that Sas-4 control peptide is wild-type (207-YASSTTASSTSPRV-220); Sas-4 mutant peptide carries two amino acid replacements TT211AA (207-YASSAAASSTSPRV-220), and Sas-4 phosphorylated peptide carries two phosphorylated threonine residues -TT211p (207-YASS**TT**ASSTSPRV-220).

(D) *In vitro* kinase assays. Plk1/Polo but not other cell-cycle kinases could phosphorylate Sas-4 control peptide used in this experiment. Note that Sas-4 mutant peptide is used in negative control experiments and phosphorylated peptide is used in positive control experiments. In control experiments, buffer replaces candidate kinases. Mitotic anti-Sas-4 antibodies (Sas-4-TT211p) were used to recognize the phosphorylation status of peptides. See also Figure S2.

(E) Plk1/Polo-mediated kinase activity is specific as revealed by the use of Plk1/Polo-kinase inhibitor BI2536, which inhibits the phosphorylation of the Sas-4 control peptide. In control experiments, the solvent DMSO replaces the inhibitor.

(F) The table summarizes the *in vitro* kinase assay using various Sas-4 peptides and mitotic kinases.

alanine. We probed these peptides using the mitotic anti-Sas-4 (Sas-4-TT211p) that is raised against two-phosphorylated threonine of Sas-4, which labels centrosomal Sas-4 only at the onset of mitosis. We noticed that the peptide (207-YASSTTASSTSPRV-220) could be phosphorylated by Plk1/Polo kinase as detected by the mitotic anti-Sas-4 (Sas-4-TT211p) (Figure 3D).

Furthermore, we could identify that Sas-4-TT211 is specifically phosphorylated by Plk1/Polo, since the antibody did not recognize the control peptide when the kinase assays used Cdk1 and aurora A (Figure 3D). The mitotic anti-Sas-4 (Sas-4-TT211p) did not recognize the peptide when -TT211 of the peptide was replaced with alanine (-TT211AA) or when the kinase assays included 1 μM BI2536, a specific Plk1/Polo inhibitor (Figure 3E). These results demonstrate that Plk1/Polo can phosphorylate Sas-4's TT211 and that mitotic anti-Sas-4 (Sas-4-TT211p) is specific for phosphorylated threonine at TT211 of Sas-4. A summary of this experiment is given in Figure 3F.

Sas-4-TT211 Seems to Be Phosphorylated at the Onset of Mitosis for an Efficient Interaction with Cnn and γ-Tubulin

To further corroborate our findings that Sas-4-TT211 is phosphorylated in cells at the onset of mitosis, we treated Schneider cells with 0.5 μM BI2536 and performed immunostaining using

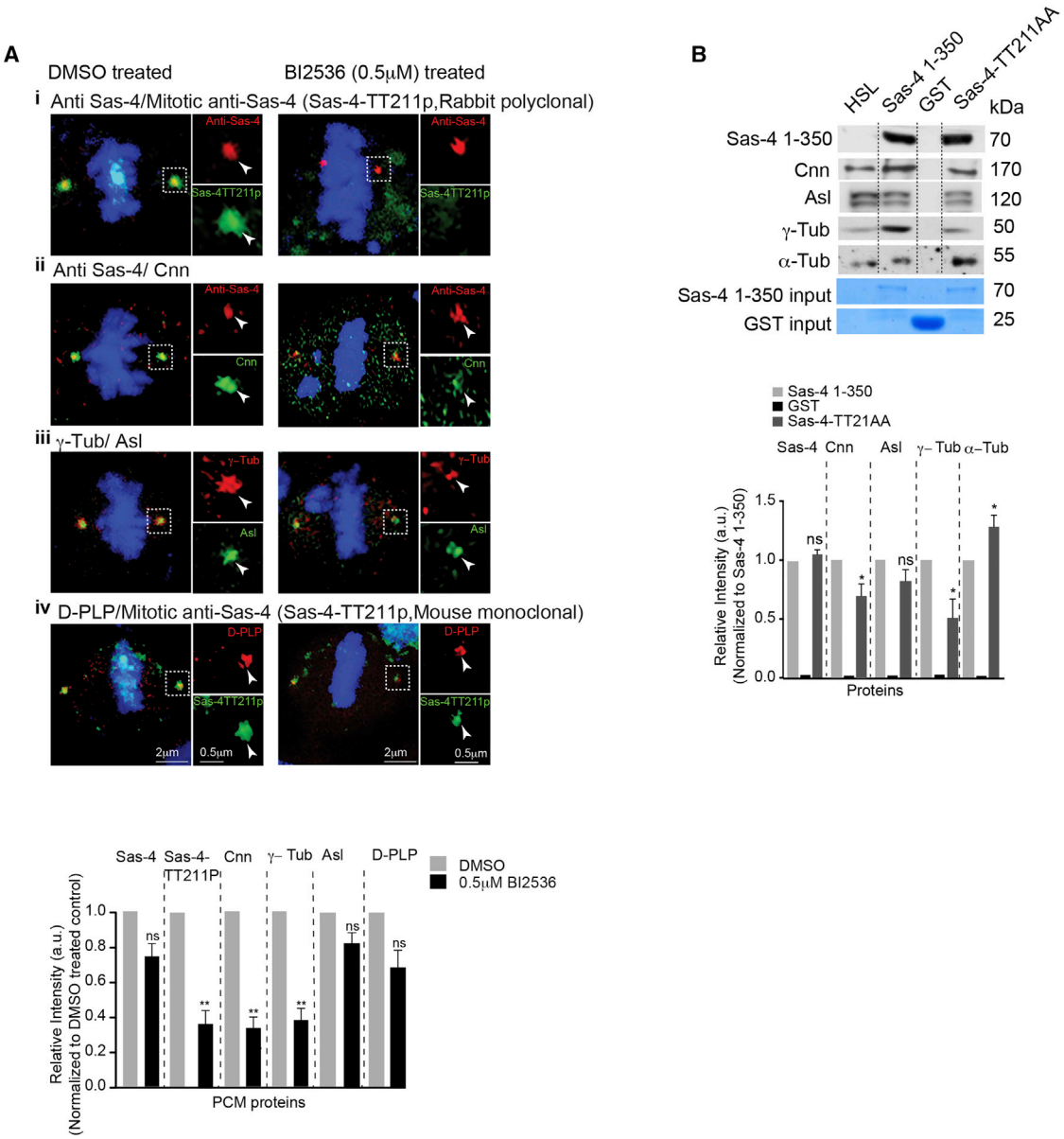

Figure 4. Phosphorylation of Sas-4-TT211 by Plk1/Polo Is Required for Efficient Binding of PCM Proteins

(A) Fraction of Schneider cells exhibiting bipolar spindles in the presence of Plk1/Polo-kinase inhibitor BI2536. In the presence of inhibitor, the mitotic anti-Sas-4 antibody (Sas-4-TT211p) fails to recognize mitotic Sas-4 (green). Note that the inhibitor BI2536 does not have the same effect on Sas-4 population that is recognized by anti-Sas-4 (red) that labels Sas-4 in all phases of the cell cycle (i). Mitotic recruitment of Cnn (green) and γ-tubulin (red) but not Asl (green) and D-PLP (red) are significantly perturbed in the presence of Plk1/Polo-kinase inhibitor BI2536 (ii–iv). The bar graph below represents the relative intensities of Sas-4, Cnn, γ-tubulin, Asl, and D-PLP recruitments to mitotic centrosomes in the presence of Plk1/Polo-kinase inhibitor BI2536. At least 60 mitotic centrosomes (n = 60) were analyzed for each condition from 3 independent experiments. Student's t test, $^{**}p < 0.001$. Error bars represent means ± SEMs.

(B) GST-pull down assay (i). Sas-4-TT211 is required for efficient binding of Cnn and γ-tubulin in the absence of endogenous Sas-4. Recombinant GST-tagged Sas-4 protein variants were used to capture its interaction partners from C131 cell extracts that lack endogenous Sas-4. HSL, high-speed cell extract that contains only cytoplasmic fractions. The bar graph at bottom represents the relative intensity of PCM proteins bound to GST-tagged Sas-4 1-350, GST, and Sas-4-TT211AA. ANOVA, $^{*}p < 0.05$. Error bars represent means ± SEMs from 3 independent experiments. See also Figure S4.

the mitotic anti-Sas-4 (Sas-4-TT211p) and anti-Sas-4 antibody. In the presence of BI2536, the mitotic anti-Sas-4 (Sas-4-TT211p) failed to strongly recognize Sas-4. In contrast, BI2536 treatment did not affect the anti-Sas-4 antibody, which labels centrosomal Sas-4 throughout the cell cycle. These data suggest that Sas-4-TT211 seems to be phosphorylated by Plk1/Polo kinase at the onset of mitosis (Figure 4A, i).

We then tested the composition of BI2536-treated mitotic centrosomes using antibodies specific for S-CAP components such as Cnn, Asl, *Drosophila* pericentrin-like protein (D-PLP),

and γ-tubulin. Analyzing a fraction of cells exhibiting bipolar spindles, we noticed that BI2536 treatment could significantly reduce the recruitment of Cnn and γ-tubulin, PCM proteins that are essential for PCM expansion in mitosis (Figure 4A, ii–iv). These data suggest that Plk1/Polo kinase activity is required to build proper mitotic centrosomes, and this could occur via the phosphorylation of Sas-4.

To investigate the importance of Sas-4-TT211 in binding PCM proteins *in vitro*, we performed glutathione S-transferase (GST) pull-down assays using recombinant Sas-4 variants (amino acids 1–350 of Sas-4) and the cytoplasmic fraction of *Drosophila* cell extracts lacking endogenous Sas-4. These cells were originally derived from *Drosophila* null embryos (Lecland et al., 2013; Zheng et al., 2014). By performing western blots for Cnn and γ-tubulin, we identified the Sas-4 variant that contains non-phosphorylatable -TT211AA, in which two threonine residues were replaced with two alanine residues, bind lesser amounts of these proteins as compared to wild-type protein. The amount of Asl binding did not vary significantly among the Sas-4 variants (Figure 4B). Thus, the finding that the recombinant Sas-4 binds S-CAP components Cnn, γ-tubulin, and Asl independently from endogenous Sas-4 reaffirms previous studies describing the ability of Sas-4 to form S-CAP complexes (Conduit et al., 2015; Gopalakrishnan et al., 2011).

Sas-4's Localization Expands Outward from Mitotic Centrosomes

Previous super-resolution microscopy studies have revealed that Sas-4 is a centriole wall protein that is closely associated with centriolar microtubules of interphase centrosomes (Dammermann et al., 2008; Gopalakrishnan et al., 2011). These studies have resolved that Sas-4 is associated with its interacting proteins D-PLP and Plk1/Polo, forming a cylinder-like zone around centrioles (Fu and Glover, 2012). To investigate the localization pattern of Sas-4 at the onset of mitosis at subdiffraction resolution, we performed STED microscopy of mitotic centrosomes of Schneider cells using our various anti-Sas-4 antibodies. Agreeing with previous findings using the anti-Sas-4 antibody, we noticed a preferential localization of Sas-4 to one of the centrioles, suggesting that they are the daughter centrioles (Figure 5A). However, imaging of mitotic centrosomes that are labeled with the mitotic anti-Sas-4 (Sas-4-TT211p) revealed an expanded localization of Sas-4 as a cloud surrounding both mother and daughter centrioles (Figure 5B). This expanded Sas-4 cloud is reminiscent of the PCM cloud labeled by Cnn and γ-tubulin, the major PCM components (Dammermann et al., 2008; Gopalakrishnan et al., 2011; Kirkham et al., 2003; Woodruff et al., 2014).

To verify this, we co-stained mitotic centrosomes with Cnn/γ-tubulin and mitotic anti-Sas-4 (Sas-4-TT211p). Cnn marked centrosomes as a cloud surrounding Sas-4 that is recognized by anti-Sas-4 (Figure 5C). However, we noticed that both the Cnn and γ-tubulin clouds co-localized with that of Sas-4, which is recognized by the mitotic anti-Sas-4 (Sas-4-TT211p) (Figures 5D and 5E). These findings indicate that phosphorylated Sas-4 at the onset of mitosis has a tendency to expand outward from mitotic centrosomes. This phenomenon is similar to that of bona fide PCM proteins such as Cnn and γ-tubulin that determine the centrosome size in mitosis.

Sas-4-TT211 Is Required for an Efficient Recruitment of Cnn and γ-Tubulin *In Vitro* and *In Vivo*

To test whether Sas-4-TT211 is essential for PCM recruitment function of Sas-4 functions *in vitro*, we expressed various Sas-4 mutations in Schneider cells and tested their ability to recruit PCM proteins to mitotic centrosomes (Figure S3). Sas-4 ΔP1-P2 expressing cells did show mild defects in Cnn recruitment, while D-PLP and Asl levels were unaffected. We reasoned that the observed mild phenotype is due to the presence of endogenous Sas-4 in Schneider cells.

We then turned to testing whether Sas-4-TT211 is essential for Sas-4 functions *in vivo*. For this, we generated transgenic *Drosophila* expressing GFP-tagged Sas-4^{WT} and Sas-4^{TT211AA}. As additional controls, we generated two different transgenic flies. GFP-tagged Sas-4$^{\Delta P1\text{-}P2}$, a larger deletion that includes both -P1 and -P2 sites, and Sas-4^{SST198AAA}, a mutation within the -P1 site harboring a threonine residue that can be phosphorylated by Cdk1 (Novak et al., 2016). All of these transgenic flies were constructed to express the Sas-4 gene under its own endogenous promoter. Except for Sas-4^{WT}, none of the Sas-4 transgenic flies harboring mutations or deletions rescued the un-coordination phenotypes of Sas-4 null flies, indicating that the perturbed regions of Sas-4 are required to form functional centrosomes.

In *Drosophila*, centrioles of matured spermatocytes elongate up to 2 μm and recruit Cnn and an enhanced level of γ-tubulin proteins only at the metaphase of male meiosis. These aspects allow fly spermatocytes to be an ideal system to analyze whether there are defects in centriole length and PCM recruitment (Gopalakrishnan et al., 2012; Zheng et al., 2016). Analyzing metaphase spermatocytes dissected from dark pupae of homozygous Sas-4 transgenic flies (Sas-4^{WT}, Sas-4^{TT211AA}, Sas-4^{SST198AAA}, and Sas-4$^{\Delta P1\text{-}P2}$ in *sas-4* null genetic background), we identified that germ cells contained the correct number of centrioles whose lengths, integrity, and configuration in a "V" shape remain unaffected (Figures S4A and S4B).

We then analyzed the ability of these centrosomes to recruit PCM proteins. We noticed that Asl or D-PLP recruitment was unaffected in all of the Sas-4 transgenic flies generated (Figures 6A, i and ii, and S4C, i). However, a proportion of cells in Sas-4^{TT211AA} and Sas-4$^{\Delta P1\text{-}P2}$ flies failed to recruit Cnn (~11% of cells in Sas-4^{TT211AA} and ~18% of cells in Sas-4$^{\Delta P1\text{-}P2}$ flies) and γ-tubulin (~9% of cells in Sas-4^{TT211AA} and ~13% of cells in Sas-4$^{\Delta P1\text{-}P2}$ flies) to at least one of the centriolar pairs.

We then analyzed a proportion of cells in which both centriolar pairs could recruit γ-tubulin and Cnn. Analyzing the intensity of Cnn and γ-tubulin recruitment revealed that compared to Sas-4^{WT} and Sas-4^{SST198AAA} flies, Sas-4^{TT211AA} and Sas-4$^{\Delta P1\text{-}P2}$ flies recruited relatively lesser amounts of Cnn and γ-tubulin (Figure 6C). We determined that, in contrast to metaphase centrosomes, interphase centrosomes could recruit normal levels of γ-tubulin (Figure S4D). Finally, we performed transmission electron microscopy of interphase and dividing spermatocytes and identified that Sas-4^{TT211AA} contained no visible structural defects in their centrioles. This finding further supports that

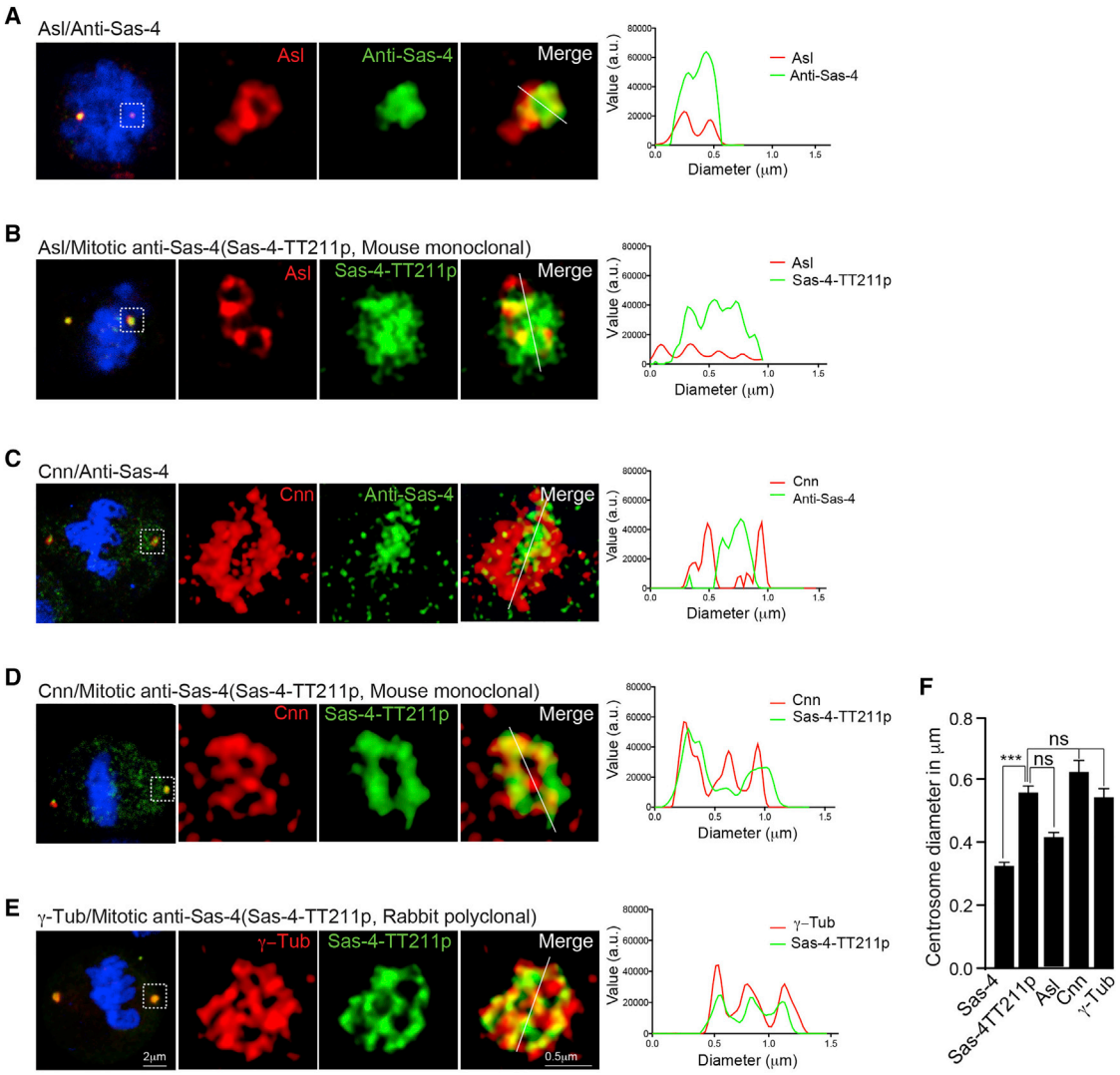

Figure 5. STED Imaging Reveals that Sas-4 Expands Outward from the Mitotic Centrosomes

(A) Localization of Sas-4 recognized by anti-Sas-4 (green) that recognizes Sas-4 throughout the cell cycle with respect to Asl (red). Note that anti-Sas-4 labels Sas-4 within a confined area.

(B) In contrast to anti-Sas-4, the mitotic-anti-Sas-4 (Sas-4-TT211p) antibody labels mitotic Sas-4 expanding outward from mitotic centrosomes (green). Asl (Red) labels both of the centrioles.

(C–E) The bona fide PCM proteins Cnn (C and D, red) and γ-tubulin (E, red) co-localize with phosphorylated Sas-4 (D and E, green). The relative diameters of centrosomal proteins are represented graphically at right.

(F) The bar graph at right represents the diameter of centrosomes distinguished by various antibodies. Note that there is no significant difference in diameter measured between phosphorylated Sas-4 and PCM proteins Cnn and γ-tubulin. At least 20 mitotic centrosomes were analyzed for each condition (n = 20). ANOVA, ***$p < 0.0001$. Error bars represent means ± SEMs.

Sas-4's TT211 is essential for PCM recruitment and does not affect the structural or numerical integrity of centrioles (Figures S5A and S5B).

Sas-4-TT211 Is Required for an Efficient Recruitment of Cnn and γ-Tubulin to Mitotic Centrosomes of Larval Brain Cells and Syncytial Embryos

Next, we tested the importance of Sas-4-TT211-mediated PCM recruitment in cell types that undergo rapid cell cycle. First, we analyzed fixed mitotic larval brain cells expressing Sas-4^{WT}, Sas-$4^{TT211AA}$, Sas-$4^{SST198AAA}$, and Sas-$4^{\Delta P1\text{-}P2}$. The mitotic cells of Sas-4^{WT} mostly contained two centrosomes, as judged by the presence of Sas-4 and Asl. In contrast, ~30% of Sas-4 mutant cells contained one centrosome (Figure S6A). Centrosomes in all cases (whether they harbor one or two centrosomes) contained nearly normal levels of Sas-4 and Asl. We then analyzed the rest of the mitotic cells that contained two centrosomes. We identified that ~30% of mitotic cells failed to efficiently recruit Cnn and γ-tubulin to at least one of the centrosomes, a phenotype that is similar to what was observed in meiotic

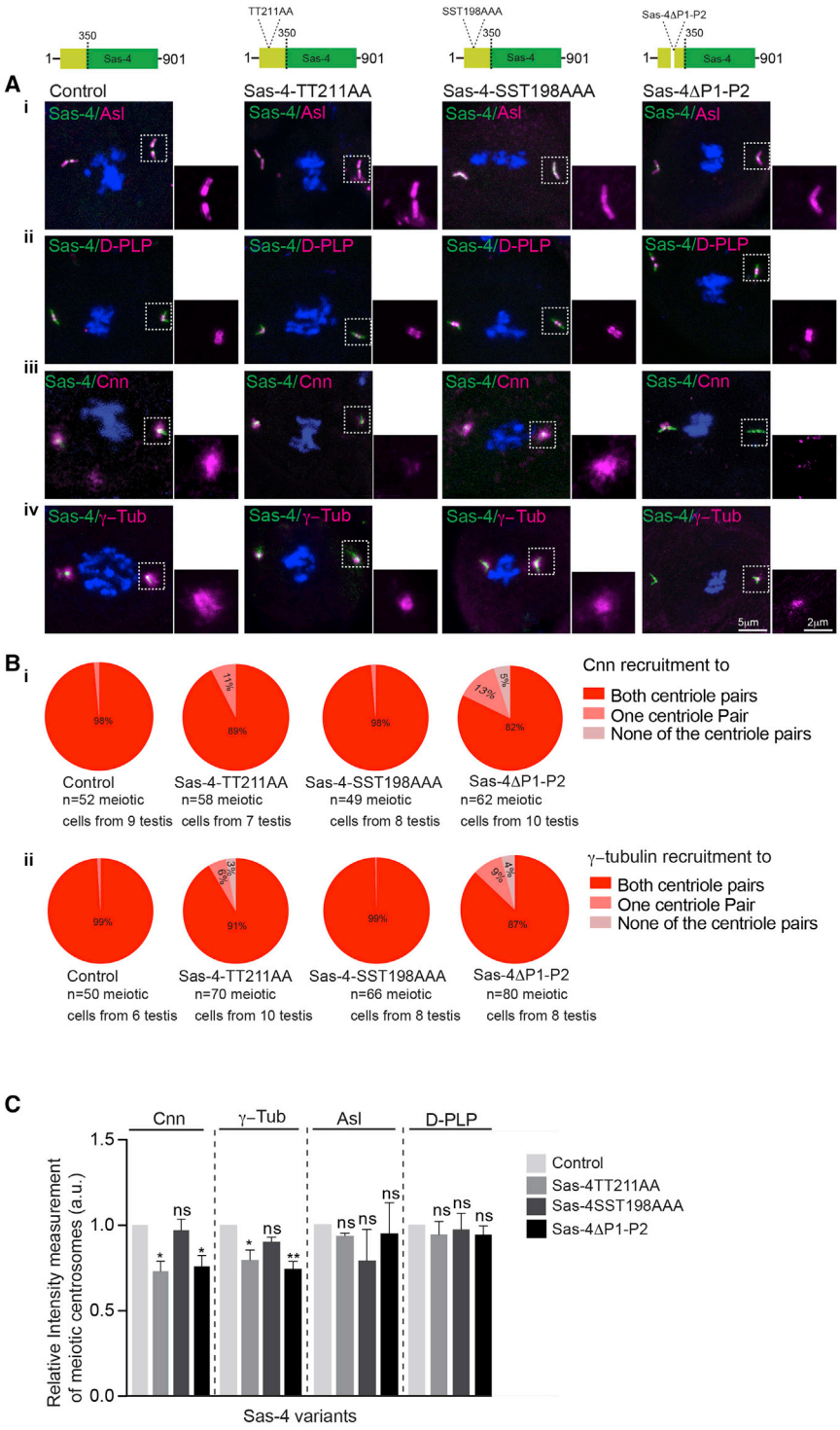

Figure 6. Sas-4-TT211 Is Required for Efficient Recruitment of PCM Proteins in Centrosomes of Meiotic Spermatocytes

(A) Asl (i, magenta) or D-PLP (ii, magenta) recruitment is unaffected in all of the transgenic flies expressing different Sas-4 variants. Cnn (iii, magenta) and γ-tubulin (iv, magenta) recruitments are reduced in Sas-4^{TT211AA} and Sas-4$^{\Delta P1\text{-}P2}$ but not in Sas-4^{SST198AAA} flies. For clarity, schematics of different Sas-4 mutations are shown at top. See also Figures S4 and S6.

(B) Pie charts represent the proportion of cells that fail to recruit Cnn (i) and γ-tubulin (ii). n represents the number of cells in each transgenic fly.

(C) Bar graph represents the relative intensities of tested proteins' recruitment to meiotic centrosomes. Note that there is a significant reduction in the recruitment of Cnn and γ-tubulin but not Asl and D-PLP in Sas-4^{TT211AA} and Sas-4$^{\Delta P1\text{-}P2}$ flies. None of these protein recruitments are affected in Sas-4^{SST198AAA} flies. At least 140 meiotic centrosomes (n = 140) from 10 testes were analyzed in each condition from 3 independent experiments. ANOVA, *$p < 0.05$, **$p < 0.001$. Error bars represent means ± SEMs.

spermatocytes (Figures S6B and S6C). Analyzing two centrosome-containing larval brain cells revealed no visible structural defects (Figure S6D).

We then continued our experiments in syncytial embryos, which are also known to undergo rapid cell division. To show the significance of phosphorylation at Sas-4-TT211, we micro-injected Sas-4-TT211p (which is the mitotic specific anti-Sas-4 antibody) to fly embryos over-expressing Cnn-red fluorescent protein (RFP). Staining centrosomes 30 min post-injection revealed a dramatic reduction in Cnn and γ-tubulin but not Asl recruitment to centrosomes that are located in the vicinity of the injection site (Figure 7). These experiments led us to conclude that an efficient recruitment of Cnn and γ-tubulin to mitotic centrosomes require Sas-4's TT211.

DISCUSSION

In this work, we identify a role for Sas-4 in building mitotic centrosomes and demonstrate how Sas-4 could be regulated at the onset of mitosis for an efficient recruitment of PCM. By using mitotic-specific anti-Sas-4 antibodies that were generated against a doubly phosphorylated threonine-containing peptide (207-YASS**TT**ASSTSPRV-220), we identify that Sas-4's -TT211 is potentially phosphorylated at the onset of mitosis (Figure 2). We then identify that Plk1/Polo is the responsible kinase that can directly interact with Sas-4 and phosphorylate at least those threonines (TT211) *in vitro*. It is known that Cnn and γ-tubulin are the bona fide PCM proteins that are required for PCM expansion during mitosis (Conduit et al.,

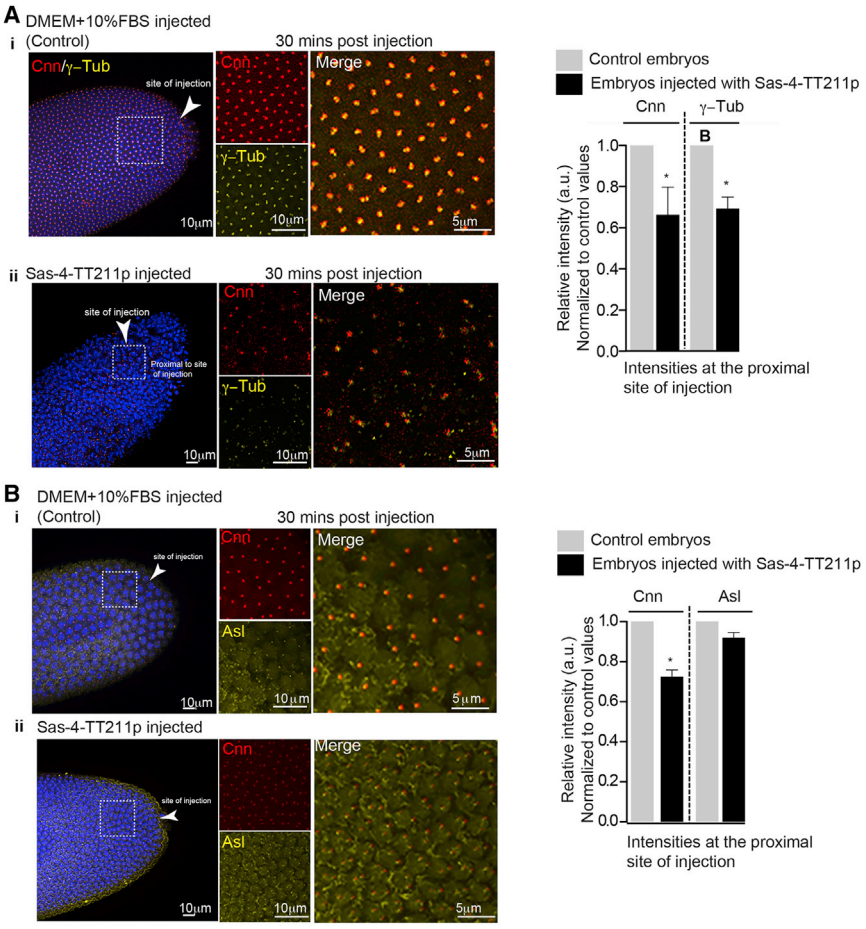

Figure 7. Phosphorylation of Sas-4-TT211 Is Required for Efficient Recruitment of Cnn and γ-Tubulin to Centrosomes of Rapidly Dividing Syncytial *Drosophila* Embryos

(A) Embryos expressing Cnn-RFP (red) under polyubiquitin promoter. Both Cnn (red) and γ-tubulin (yellow) do not seem to be affected in embryos injected with 10% fetal bovine serum (FBS) (i). Sas-4-TT211p injected embryos (ii) show dramatic reduction in both Cnn and γ-tubulin 30 min post-injection. Bar graphs represent the relative intensities of PCM proteins at mitotic centrosomes. At least 120 mitotic centrosomes (n = 120) from 4 embryos were analyzed in each condition. ANOVA, *p < 0.05. Error bars represent means ± SEMs. See also Figures S3, S4, and S6. (B) Asl (yellow) recruitment does not seem to significantly change in embryos injected with Sas-4-TT211p antibody (i and ii). Bar graphs represent the relative intensities of PCM proteins at mitotic centrosomes. At least 80 mitotic centrosomes (n = 80) from 4 embryos were analyzed in each condition. ANOVA, *p < 0.05. Error bars represent means ± SEMs.

2014; Gopalakrishnan et al., 2011; Sunkel et al., 1995). Our *in vivo* studies using *Drosophila* spermatocytes, brain cells, and syncytial embryos reveal the importance of Sas-4-TT211 in PCM expansion in dividing cells.

Plk1/Polo kinase is critical for the process of PCM recruitment (Kong et al., 2014; Wang et al., 2011). The number of Plk1/Polo substrates has been identified, which include Cnn, SPD-5, and D-PLP (Conduit and Raff, 2010; Woodruff et al., 2015; Wueseke et al., 2016). However, the significance of Plk1/Polo-mediated phosphorylation precisely at the onset of mitosis has largely been unexplored. The identification of Sas-4 as a Plk1/Polo substrate provides further insights into this process. Based on our data, it appears that phosphorylation of Sas-4-TT211 precedes the further recruitment of PCM proteins to mitotic centrosomes. This could be explained by the fact that Sas-4 is a closely associated centriolar wall protein whose phosphorylation could trigger Sas-4 to recruit subsequent PCM proteins and expand the overall size of centrosomes in mitosis. If this is true, then it is formally expected that upon phosphorylation, Sas-4 protein could remodel its own localization, spreading outward from its original location. Our STED microscopy using mitotic anti-Sas-4 antibodies (both mouse monoclonal and rabbit polyclonal Sas-4-TT211p) demonstrate an expanded localization of Sas-4 in mitotic centrosomes (Figure 5).

Our experiments further support the idea that Sas-4 is a crucial player at the early events of PCM recruitment. First, PCM recruitment begins at the onset of mitosis where Sas-4 appears to be phosphorylated by Plk1/Polo kinase (Figure 3). Second, our *in vivo* experiments using *Drosophila* that express a mildly perturbed Sas-4 (Sas-4^{TT211AA}) is sufficient to cause PCM recruitment defects in significant numbers of meiotic and mitotic centrosomes (Figures 6 and S6). Although the penetrance of the mutation seems to be minimal in slow-dividing spermatocytes, it is noteworthy that a fraction of affected centriolar pairs completely failed to recruit Cnn and γ-tubulin (Figures 6A, iii and iv, 6B, and S4C, ii and iii).

The centrosomes of Sas-4^{TT211AA} could recruit Asl but not Cnn and γ-tubulin sufficiently. This finding also suggests that PCM expansion at the onset of mitosis is to some extent dependent on the phosphorylation status of Sas-4 but not Asl. Novak et al. (2016) identified that PCM recruitment is dependent on the phosphorylation status of Sas-4. However, our findings contradict their observation that Cnn recruitment is Asl dependent. Few of our mutant flies, which encompass the Cdk1 site examined by Novak and colleagues, could normally recruit Asl (Figures 6 and S6). Although these studies provide key insights into the PCM recruitment process, the results offer a re-examination of the role of Asl in PCM recruitment. One remote possibility to explain these contrasting findings could be differences in expression levels, genetic background, and centrosome assembly mechanisms in various tissues, which are yet to be solved (Conduit and Raff, 2015).

Based on our data, it is likely that phosphorylated Sas-4 has a high affinity for PCM proteins in mitosis. The same phenomenon is observed for centrosomal P4.1-associated protein (CPAP), the

human counterpart of Sas-4, which acquires a high affinity for PCM proteins upon phosphorylation (Chou et al., 2016). Although our findings reveal that significant numbers of Sas-4^{TT211AA} and Sas-4$^{\Delta P1\text{-}P2}$ centrosomes have defects in Cnn and γ-tubulin recruitment, we notice that a certain proportion of centrosomes could still recruit a residual amount of these proteins (Figures 6 and S6). This observation suggests that Sas-4 could additionally contain Plk1/Polo kinase sites other than TT211 or involve other PCM recruitment mechanisms that are operating independently of Sas-4.

Until recently, the consequences regarding centrosomes that fail to efficiently recruit PCM proteins remain unanswered and numerous interpretations are possible. It is likely that centrosomes that are incapable of recruiting the full complement of PCM proteins fail to duplicate or to undergo centriole-to-centrosome conversion in subsequent cell divisions, as recently demonstrated by Fu et al. (2016) and Novak et al. (2016). This phenomenon is reflected in our studies that ~30% of mitotic cells in Sas-4^{TT211AA} and Sas-4$^{\Delta P1\text{-}P2}$ larval brain exhibit only one centrosome, as judged by the presence of Sas-4 or Asl proteins. This could indirectly mean that Sas-4^{TT211AA} and Sas-4$^{\Delta P1\text{-}P2}$ centrosomes that fail to recruit the full complement of PCM components are non-functional and are incapable of undergoing centriole-to-centrosome conversion in subsequent cell divisions. If this is true, then our findings here also suggest that the phenomenon of centriole-to-centrosome conversion seems to occur only in cell types that undergo rapid cell cycling, in which an efficient centrosome function is indispensable. This is substantiated by our experiments that analyze meiotic spermatocytes that have a much longer cell cycle. Despite Sas-4^{TT211AA} and Sas-4$^{\Delta P1\text{-}P2}$ expressing meiotic spermatocyte centrosomes failing to efficiently recruit PCM proteins, we never noticed single centrosome-containing cells (Figure S4A).

In summary, our experiments dissect Sas-4's function in meiotic and mitotic PCM recruitment in diverse cell types independent from its role in centriole elongation and duplication. Thus, the present data add useful insights into early events of PCM recruitment that occur at the onset of mitosis. Although great progress has been made in dissecting the order of S-CAP components' (Sas-4, Cnn, Asl, γ-tubulin, and D-PLP) recruitment to mitotic centrosomes, to what extent individual S-CAP components contribute to build functional mitotic centrosomes remains elusive. *In vitro* functional reconstitution assays of centrosomes using purified endogenous protein complexes from cell extracts depleted with individual S-CAP components may provide useful insights into the complex process of PCM recruitment in building functional centrosomes.

STAR★METHODS

Detailed methods are provided in the online version of this paper and include the following:

- KEY RESOURCES TABLE
- CONTACT FOR REAGENT AND RESOURCE SHARING
- EXPERIMENTAL MODEL AND SUBJECT DETAILS
  - Drosophila melanogaster
  - *Drosophila* Schneider cells and Sas-4 null cells (C131)
- METHOD DETAILS
  - Plasmids and cloning
  - Cell Culture and transfection
  - Antibody generation
  - Antibodies
  - Antibody injection in *Drosophila* embryos
  - Immunofluorescence and light microscopy
  - Electron microscopy
  - Peptide generation and dot blot analysis
  - *In vitro* kinase assay
  - Antibody competition experiment
  - Recombinant protein purification
  - GST Pull-down assays
  - Immunoprecipitation (IP) of Sas-4 complexes
  - Western blotting and Coomassie staining
- QUANTIFICATION AND STATISTICAL ANALYSIS

SUPPLEMENTAL INFORMATION

Supplemental Information includes six figures and can be found with this article online at https://doi.org/10.1016/j.celrep.2018.11.102.

ACKNOWLEDGMENTS

The Deutsche Forschungsgemeinschaft (DFG) grant GO 2301/2-2 and the Human Frontier Science Program (HFSP) (RGY0064/2015) supported this work. We would like to thank the members of the Laboratory for Centrosome and Cytoskeleton Biology for their technical support and advice. We also thank the light microscopy facility of the CMMC/CECAD, University of Cologne.

AUTHOR CONTRIBUTIONS

Conceptualization, J.G.; Methodology, A.R. and J.G.; Investigation, A.R.; Investigation (light microscopy, molecular biology, and biochemical analysis), A.R. and A.M.; Investigation (bioinformatics), S.M. and H.U.; Resources, A.D. and R.F.; Investigation (electron microscopy), M.G., M.R., G.C.; Writing, Editing, & Supervision, A.R., J.G., and A.M.; Funding Acquisition, J.G. All of the authors listed here have contributed to the preparation of this manuscript.

DECLARATION OF INTERESTS

The authors declare no competing interests.

Received: December 6, 2017
Revised: September 19, 2018
Accepted: November 29, 2018
Published: December 26, 2018

REFERENCES

Asteriti, I.A., De Mattia, F., and Guarguaglini, G. (2015). Cross-Talk between AURKA and Plk1 in Mitotic Entry and Spindle Assembly. Front. Oncol. *5*, 283.

Avidor-Reiss, T., and Gopalakrishnan, J. (2013). Building a centriole. Curr. Opin. Cell Biol. *25*, 72–77.

Blachon, S., Gopalakrishnan, J., Omori, Y., Polyanovsky, A., Church, A., Nicastro, D., Malicki, J., and Avidor-Reiss, T. (2008). Drosophila asterless and vertebrate Cep152 Are orthologs essential for centriole duplication. Genetics *180*, 2081–2094.

Chou, E.J., Hung, L.Y., Tang, C.J., Hsu, W.B., Wu, H.Y., Liao, P.C., and Tang, T.K. (2016). Phosphorylation of CPAP by Aurora-A Maintains Spindle Pole Integrity during Mitosis. Cell Rep. *14*, 2975–2987.

Conduit, P.T., and Raff, J.W. (2010). Cnn dynamics drive centrosome size asymmetry to ensure daughter centriole retention in Drosophila neuroblasts. Curr. Biol. *20*, 2187–2192.

Conduit, P.T., and Raff, J.W. (2015). Different Drosophila cell types exhibit differences in mitotic centrosome assembly dynamics. Curr. Biol. *25*, R650–R651.

Conduit, P.T., Brunk, K., Dobbelaere, J., Dix, C.I., Lucas, E.P., and Raff, J.W. (2010). Centrioles regulate centrosome size by controlling the rate of Cnn incorporation into the PCM. Curr. Biol. *20*, 2178–2186.

Conduit, P.T., Richens, J.H., Wainman, A., Holder, J., Vicente, C.C., Pratt, M.B., Dix, C.I., Novak, Z.A., Dobbie, I.M., Schermelleh, L., and Raff, J.W. (2014). A molecular mechanism of mitotic centrosome assembly in Drosophila. eLife *3*, e03399.

Conduit, P.T., Wainman, A., Novak, Z.A., Weil, T.T., and Raff, J.W. (2015). Re-examining the role of Drosophila Sas-4 in centrosome assembly using two-colour-3D-SIM FRAP. eLife *4*, e08483.

Dammermann, A., Maddox, P.S., Desai, A., and Oegema, K. (2008). SAS-4 is recruited to a dynamic structure in newly forming centrioles that is stabilized by the gamma-tubulin-mediated addition of centriolar microtubules. J. Cell Biol. *180*, 771–785.

Dix, C.I., and Raff, J.W. (2007). Drosophila Spd-2 recruits PCM to the sperm centriole, but is dispensable for centriole duplication. Curr. Biol. *17*, 1759–1764.

Fish, M.P., Groth, A.C., Calos, M.P., and Nusse, R. (2007). Creating transgenic Drosophila by microinjecting the site-specific phiC31 integrase mRNA and a transgene-containing donor plasmid. Nat. Protoc. *2*, 2325–2331.

Fu, J., and Glover, D.M. (2012). Structured illumination of the interface between centriole and peri-centriolar material. Open Biol. *2*, 120104.

Fu, J., Lipinszki, Z., Rangone, H., Min, M., Mykura, C., Chao-Chu, J., Schneider, S., Dzhindzhev, N.S., Gottardo, M., Riparbelli, M.G., et al. (2016). Conserved molecular interactions in centriole-to-centrosome conversion. Nat. Cell Biol. *18*, 87–99.

Giansanti, M.G., Bucciarelli, E., Bonaccorsi, S., and Gatti, M. (2008). Drosophila SPD-2 is an essential centriole component required for PCM recruitment and astral-microtubule nucleation. Curr. Biol. *18*, 303–309.

Gopalakrishnan, J., Mennella, V., Blachon, S., Zhai, B., Smith, A.H., Megraw, T.L., Nicastro, D., Gygi, S.P., Agard, D.A., and Avidor-Reiss, T. (2011). Sas-4 provides a scaffold for cytoplasmic complexes and tethers them in a centrosome. Nat. Commun. *2*, 359.

Gopalakrishnan, J., Chim, Y.C., Ha, A., Basiri, M.L., Lerit, D.A., Rusan, N.M., and Avidor-Reiss, T. (2012). Tubulin nucleotide status controls Sas-4-dependent pericentriolar material recruitment. Nat. Cell Biol. *14*, 865–873.

Haren, L., Stearns, T., and Lüders, J. (2009). Plk1-dependent recruitment of gamma-tubulin complexes to mitotic centrosomes involves multiple PCM components. PLoS One *4*, e5976.

Hung, L.Y., Chen, H.L., Chang, C.W., Li, B.R., and Tang, T.K. (2004). Identification of a novel microtubule-destabilizing motif in CPAP that binds to tubulin heterodimers and inhibits microtubule assembly. Mol. Biol. Cell *15*, 2697–2706.

Kirkham, M., Müller-Reichert, T., Oegema, K., Grill, S., and Hyman, A.A. (2003). SAS-4 is a C. elegans centriolar protein that controls centrosome size. Cell *112*, 575–587.

Kong, D., Farmer, V., Shukla, A., James, J., Gruskin, R., Kiriyama, S., and Loncarek, J. (2014). Centriole maturation requires regulated Plk1 activity during two consecutive cell cycles. J. Cell Biol. *206*, 855–865.

Lawo, S., Hasegan, M., Gupta, G.D., and Pelletier, L. (2012). Subdiffraction imaging of centrosomes reveals higher-order organizational features of pericentriolar material. Nat. Cell Biol. *14*, 1148–1158.

Lecland, N., Debec, A., Delmas, A., Moutinho-Pereira, S., Malmanche, N., Bouissou, A., Dupré, C., Jourdan, A., Raynaud-Messina, B., Maiato, H., and Guichet, A. (2013). Establishment and mitotic characterization of new Drosophila acentriolar cell lines from DSas-4 mutant. Biol. Open *2*, 314–323.

Mennella, V., Agard, D.A., Huang, B., and Pelletier, L. (2014). Amorphous no more: subdiffraction view of the pericentriolar material architecture. Trends Cell Biol. *24*, 188–197.

Nigg, E.A. (2004). Centrosomes in Development and Disease (Wiley-VCH).

Nigg, E.A., and Holland, A.J. (2018). Once and only once: mechanisms of centriole duplication and their deregulation in disease. Nat. Rev. Mol. Cell Biol. *19*, 297–312.

Nigg, E.A., and Raff, J.W. (2009). Centrioles, centrosomes, and cilia in health and disease. Cell *139*, 663–678.

Novak, Z.A., Conduit, P.T., Wainman, A., and Raff, J.W. (2014). Asterless licenses daughter centrioles to duplicate for the first time in Drosophila embryos. Curr. Biol. *24*, 1276–1282.

Novak, Z.A., Wainman, A., Gartenmann, L., and Raff, J.W. (2016). Cdk1 Phosphorylates Drosophila Sas-4 to Recruit Polo to Daughter Centrioles and Convert Them to Centrosomes. Dev. Cell *37*, 545–557.

Riparbelli, M.G., Gottardo, M., Glover, D.M., and Callaini, G. (2014). Inhibition of Polo kinase by BI2536 affects centriole separation during Drosophila male meiosis. Cell Cycle *13*, 2064–2072.

Sunkel, C.E., Gomes, R., Sampaio, P., Perdigão, J., and González, C. (1995). Gamma-tubulin is required for the structure and function of the microtubule organizing centre in Drosophila neuroblasts. EMBO J. *14*, 28–36.

Tang, N., and Marshall, W.F. (2012). Centrosome positioning in vertebrate development. J. Cell Sci. *125*, 4951–4961.

Wang, W.J., Soni, R.K., Uryu, K., and Tsou, M.F. (2011). The conversion of centrioles to centrosomes: essential coupling of duplication with segregation. J. Cell Biol. *193*, 727–739.

Woodruff, J.B., Wueseke, O., and Hyman, A.A. (2014). Pericentriolar material structure and dynamics. Philos. Trans. R. Soc. Lond. B Biol. Sci. *369*, 20130459.

Woodruff, J.B., Wueseke, O., Viscardi, V., Mahamid, J., Ochoa, S.D., Bunkenborg, J., Widlund, P.O., Pozniakovsky, A., Zanin, E., Bahmanyar, S., et al. (2015). Centrosomes. Regulated assembly of a supramolecular centrosome scaffold in vitro. Science *348*, 808–812.

Wueseke, O., Zwicker, D., Schwager, A., Wong, Y.L., Oegema, K., Jülicher, F., Hyman, A.A., and Woodruff, J.B. (2016). Polo-like kinase phosphorylation determines Caenorhabditis elegans centrosome size and density by biasing SPD-5 toward an assembly-competent conformation. Biol. Open *5*, 1431–1440.

Zheng, X., Gooi, L.M., Wason, A., Gabriel, E., Mehrjardi, N.Z., Yang, Q., Zhang, X., Debec, A., Basiri, M.L., Avidor-Reiss, T., et al. (2014). Conserved TCP domain of Sas-4/CPAP is essential for pericentriolar material tethering during centrosome biogenesis. Proc. Natl. Acad. Sci. USA *111*, E354–E363.

Zheng, X., Ramani, A., Soni, K., Gottardo, M., Zheng, S., Ming Gooi, L., Li, W., Feng, S., Mariappan, A., Wason, A., et al. (2016). Molecular basis for CPAP-tubulin interaction in controlling centriolar and ciliary length. Nat. Commun. *7*, 11874.

STAR★METHODS

KEY RESOURCES TABLE

REAGENT or RESOURCE	SOURCE	IDENTIFIER
Antibodies		
DAPI	Sigma Aldrich	Cat# 32670
Donkey anti rabbit IgG (H+L) secondary antibody, Alexa Fluor 594	Life Technologies	Cat# A21207
Donkey anti rabbit IgG (H+L) secondary antibody, Alexa Fluor 647	Life Technologies	Cat# A31573
Donkey anti-Rabbit IgG (H+L) Secondary Antibody, HRP	Thermoscientific	Cat# A16023
Goat anti mouse IgG (H+L) secondary antibody, Alexa Fluor 488	Life Technologies	Cat# A28175
Goat anti mouse IgG (H+L) secondary antibody, Alexa Fluor 594	Life Technologies	Cat# A-11032
Goat anti mouse IgG (H+L) secondary antibody, Alexa Fluor 647	Life Technologies	Cat# A21236
Goat anti-Mouse IgG (H+L) Secondary Antibody, HRP	Thermoscientific	Cat# 626520
Monoclonal mouse anti-α-Tubulin	Sigma Aldrich	Cat# T9026, Clone DM1A
Monoclonal mouse anti-γ-tubulin	Sigma Aldrich	Cat# GTU-88
Mouse monoclonal anti-phospho-Histone H3, Ser10	Cell Signaling technologies	Cat# 6G3
Mouse monoclonal anti-Sas-4	N/A	(Gopalakrishnan et al., 2011)
Mouse monoclonal mitotic anti-Sas-4	Generated for this paper	N/A
Mouse monoclonal non-mitotic anti Sas-4	Self generated for this paper	N/A
Rabbit polyclonal anti-Asl	N/A	(Blachon et al., 2008)
Rabbit polyclonal anti-Cnn	Kind gift from Dr. T. Kaufman	N/A
Rabbit polyclonal anti-D-PLP	Kind gift from Dr. J. Raff	N/A
Rabbit polyclonal mitotic anti-Sas-4	Generated at Genscript	N/A
Bacterial strains		
BL21 (DE3) competent *E. coli*	New England Biolabs	Cat# C2527I
NEB 5 alpha competent *E. coli*	New England Biolabs	Cat# C2987I
Chemicals		
37% Formaldehyde	Sigma Aldrich	Cat# F8775
BI2536	Selleckchem	Cat# S1109
Bovine serum albumin	Sigma Aldrich	Cat# A7906-100G
Concanavalin A	Sigma Aldrich	Cat# C0412-5MG
Coomassie Brillant blue G-250 (C. I. 42655)	Applichem	Cat# A3480,0025
Drosophila Schneider medium	Thermo Fischer Scientific	Cat# 21720024
Hi load 16/600 Superdex 200pg	GE Healthcare	Cat# 28-9893-35
Fetal Bovine serum (Sterile filtered)	VWR	Cat# S1810-500
Glacial acetic acid	ROTH	Cat# 3738.3
Glutaraldehyde EM Grade, 50% Aqueous Solution	Science services	Cat# E16300
Glutathione Sepharose 4 Fast flow (GST)	GE Healthcare	Cat# 17-5132-01
Protein G Sepharose 4 fast flow	GE Healthcare	Cat# 17-0618-01
Glycerol > 99% molecular biology grade	Sigma Aldrich	Cat# G5516-1L
Guanidine hydrochloride	ROTH	Cat# 35.1
Isopropylthiogalactoside (IPTG)	Sigma aldrich	Cat# I6758-1G
Methanol Rotipuran > 99.9% ACS ISO	ROTH	Cat# 4627.5
Mowiol 4-88 Histology grade	Applichem	Cat# A9011,0100
Heptane anhydrous 99%	Sigma Aldrich	Cat# 246654-1L
Non-fat dried milk powder	Applichem	Cat# A80830,1000
Osmium Tetroxide, Crystalline, Highest Purity 99,95%	Science services	Cat# E19120
Penicillin-Streptomycin (100x)	Thermofischer scientific	Cat# 15140-122

(*Continued on next page*)

Continued

REAGENT or RESOURCE	SOURCE	IDENTIFIER
Shields and Sang M3 insect medium	Sigma Aldrich	Cat# S3652
Sodium chloride	Applichem	Cat# A1149,5000
Pipes dipotasium salt	Sigma Aldrich	Cat# P7643-500G
Supersignal West Femto Chemiluminescent substrate	Thermofischer scientific	Cat# 34095
Supersignal West Pico Chemiluminescent substrate	Thermofischer scientific	Cat# 34080
PBS tablets	GIBCO	Cat#18912-014
Tris Ultrapure	Applichem	Cat# A1086,1000
Triton X-100	Applichem	Cat# A13880500
Tween-20	Applichem	Cat# A1389,1000
Peptides		
Sas-4 Control peptide (YASSTTASSTSPRV)	Generated at Genscript for this paper	N/A
Sas-4 double mutant peptide (YASSAAASSTSPRV)	Generated at Genscript for this paper	N/A
Sas-4 double phospho peptide (YASSpTpTASSTSPRV)	Generated at Genscript for this paper	N/A
Sas-4 single mutant peptide #1 YAASTTASSTSPRV)	Generated at Genscript for this paper	N/A
Sas-4 single mutant peptide #2 YASATTASSTSPRV)	Generated at Genscript for this paper	N/A
Sas-4 single mutant peptide #3 YASSATASSTSPRV)	Generated at Genscript for this paper	N/A
Sas-4 single mutant peptide #4 YASSTAASSTSPRV)	Generated at Genscript for this paper	N/A
Recombinant Proteins		
Recombinant human PLK1	Proqinase	Cat# 0183-0000-1
Recombinant Aurora A kinase	Proqinase	Cat# 0166-0000-1
Recombinant CDK1/CycA2	Proqinase	Cat# 0134-0054-1
Recombinant Sas-4(1-350)ΔP1-P2	This Paper	N/A
Recombinant Sas-4(1-350) SST198DDD	This Paper	N/A
Recombinant Sas-4(1-350) SST198AAA	This Paper	N/A
Recombinant Sas-4(1-350) SSTT209DDDD	This Paper	N/A
Recombinant Sas-4(1-350) SSTT209AAAA	This Paper	N/A
Recombinant Sas-4(1-350) TT211AA	This Paper	N/A
Critical Commercial Assays		
Effectene Transfection reagent	QIAGEN	Cat# 301425
Phusion High- Fedality DNA polymerase	New England Biolabs	Cat# M0530L
Experimental Models: Cell Lines		
Drosophila Schneider cells	Kind gift from Prof. Linda Partridge	N/A
Drosophila Sas-4 null cells (C131)	(Zheng et al., 2014)	N/A
Experimental Models: Organisms/Strains		
*D.*melanogaster P[lacW]l(3)s2214 (Sas-4^{s2214})	Bloomington	(Zheng et al., 2014)
D.melanogaster p-Ubq RFP-Cnn (II chromosome)	Kind Gift from Prof. Jorden Raff	N/A
W^{+}; Sas-4/Cyo; Sas-4 s^{2214}/ Sas-4^{s2214}	BestGene(USA)	N/A
W^{+}; Sas-4 $^{\Delta P1\text{-}P2}$ /Cyo; Sas-4 s^{2214}/ Sas-4^{s2214}	BestGene(USA)	N/A
W^{+}; Sas-4^{SST198AAA}/Cyo; Sas-4^{s2214}/ Sas-4^{s2214}	BestGene(USA)	N/A
W^{+}; Sas-4^{TT211AA} /Cyo; Sas-4 s^{2214}/ Sas-4^{s2214}	BestGene(USA)	N/A
W^{+}; Sas-4^{TT211DD} /Cyo; Sas-4 s^{2214}/ Sas-4^{s2214}	BestGene(USA)	N/A

(*Continued on next page*)

Continued		
REAGENT or RESOURCE	SOURCE	IDENTIFIER
Oligonucleotides		
Sas-4 Genomic forward primer GGCGCGCCTATTTTTTGAATCA TAAATGATTAA	Sigma Aldrich	N/A
Sas-4 Genomic Reverse primer GCGGCCGCCTAATACTTGGC ATAGTCTGTGTC	Sigma Aldrich	N/A
Sas-4 1-350 CDS Forward primer GGAATTCCATATGCAGGAG GCTGGCGAAAGTCCTGTTGGA	Sigma Aldrich	N/A
Sas-4 1-350 CDS Reverse primer TTCCGCGGCCGCTATGGCC GACGTCGACCTCGTCCCCCTCCTGCAGTTCCTGC	Sigma Aldrich	N/A
Recombinant DNA		
PattB-UAST vector	(Zheng et al., 2014)	N/A
pGEX-6P-1	Kind Gift from Prof. Haitao Li.	N/A
Software and Algorithms		
Fiji Win64 (ImageJ d 1.47)	Wayne Rasband, NIH, USA	N/A
Adobe Illustrator CC 2017	Adobe	N/A
Adobe Photoshop CC 2015	Adobe	N/A
Huygens for image deconvolution	Scientific Volume Imaging	N/A

CONTACT FOR REAGENT AND RESOURCE SHARING

Jay Gopalakrishnan (Institute of Human Genetics, Heinrich-Heine-Universität Düsseldorf) is the lead contact for this paper and is responsible for any reagent and resource request. Enquiries should be sent to Jay Gopalakrishnan (jay.gopalakrishnan@hhu.de).

EXPERIMENTAL MODEL AND SUBJECT DETAILS

Drosophila melanogaster

P[lacW]l(3)s2214 (Sas-4s2214) was obtained from the Bloomington Stock Center. Sas-4^{WT}, Sas-4^{TT211AA}, Sas-4^{TT211DD} Sas-4^{SST198AAA} and Sas-4 $^{\Delta P1\text{-}P2}$ were cloned into pUAST-attb-GFP vector and sent to BestGene(USA) for generating transgenic flies. All the genes were expressed under Sas-4 endogenous promoter and were inserted at the identical sites in the second chromosome. The flies obtained were balanced to generate stable stocks. Each of the Sas-4 transgenic flies were expressed in the background of Sas-4 null homozygous mutation. The generated flies have been listed in the key resource table.

Drosophila Schneider cells and Sas-4 null cells (C131)

Drosophila Schneider cells were cultured in Schneider's *Drosophila* medium (Thermo Fischer Scientific) containing 10% fetal bovine serum (Bio-west) and the *Drosophila* cells lacking Sas-4 (Zheng et al., 2014) were cultured in Shields and Sang M3 insect medium (Sigma Aldrich) containing 10% fetal bovine serum (Bio-west). The cells were grown at 25°C and split 1/3 once every 4 days.

METHOD DETAILS

Plasmids and cloning

Full length Sas-4-WT (control), Sas-4-TT211AA, Sas-4-TT211DD, Sas-4-SST198AAA, and Sas-4 ΔP1-P2 genes were amplified from *Drosophila* genomic DNA and cloned into PattB-UAST-GFP (C-terminal GFP) vector between AscI and NotI cloning sites under endogenous Sas-4 promoter for generating transgenic *Drosophila*. The Sas-4 variants (as stated above) spanning 1-350aa residues were amplified using Phusion polymerase (NEB) and cloned into pGEX-6p1 vector between NdeI and SalI for protein expression and purification. The genes consisted of fused N-terminal GST tag for purification purposes.

Cell Culture and transfection

Drosophila Schneider cells were cultured in Schneider's *Drosophila* medium (Thermo Fischer Scientific) containing 10% fetal bovine serum (Bio-west) and the *Drosophila* cells lacking Sas-4 were cultured in Shields and Sang M3 insect medium. The cells were split 1/3 once every 4 days. Transfection in *Drosophila* S2 cells was carried out using the Effectene transfection reagent (QIAGEN) as per the manufacturer's protocol.

Antibody generation

Non-mitotic anti-Sas-4 was generated by injecting mice with Sas-4 peptide (150-300aa). Later the epitope for the antibody was narrowed down to the peptide sequence spanning 190-220aa (refer to Figure 1A). Mouse monoclonal mitotic anti-Sas-4 (Sas-4-TT211p) was raised against a phosphorylated peptide (207-YASSpTpTASSTSPRV-220, generated by GenScript, NJ, USA) (refer to Figures 2B and S1F).

Antibodies

For immunofluorescence, monoclonal mouse anti-Sas-4 (1:50)(Gopalakrishnan et al., 2011) mouse non-mitotic anti-Sas-4 (1:50, generated in our lab), mouse mitotic anti-Sas-4 (Sas-4-TT211p, 1:2, generated in our lab), rabbit mitotic anti-Sas-4 (Sas-4-TT211p, 1:100, GenScript), rabbit anti-Asl (1:500)(Blachon et al., 2008), rabbit anti-Cnn (1:500, courtesy of Dr. T. Kaufman), rabbit anti-D-PLP (1:500, Courtesy of Dr. J. Raff), mouse anti-γ-tubulin (1:400, Sigma aldrich) and mouse anti-phospho-Histone H3, Ser10 (1:250, Cell Signaling Technology) were used. DAPI (1 μg/ml. Sigma) was used to stain DNA. Secondary antibodies, Alexa fluor dyes (goat or donkey anti-mouse/ anti-rabbit) were used at 1:1000 dilution (Life technologies). For STED imaging, Abberior STAR dyes (anti-mouse 647 and anti-rabbit 594) were used.

For western blotting and dot blot analysis, monoclonal mouse anti-Sas-4 (1:100)(Gopalakrishnan et al., 2011) mouse non-mitotic anti-Sas-4 (1:100, generated in out lab), mouse monoclonal mitotic anti-Sas-4 (Sas-4-TT211p, 1:10), rabbit polyclonal mitotic anti-Sas-4 (Sas-4-TT211p, 1:1000, GenScript), rabbit anti-Asl (1:3000)(Blachon et al., 2008) rabbit anti-Cnn (1:3000, courtesy of Dr. T. Kaufman), mouse anti-γ-tubulin (1:3000, Sigma aldrich) mouse anti-α-tubulin (1:3000, Sigma Aldrich), rabbit anti-α-tubulin (1:3000, courtesy of Prof. Dr. Angelika A. Noegel) and rabbit anti-Human Plk1 (1:1000, NEB) were used. Secondary antibodies (anti-mouse and anti-rabbit) (1:5000, Thermo Fischer Scientific) were used.

Antibody injection in *Drosophila* embryos

Drosophila flies expressing Cnn-RFP under poly-ubiquitin promoter were allowed to lay eggs on grape juice agar medium for 1-week prior to injection at 25°C. The flies were flipped to new plate once every 24 hr. 1hr old syncytial embryos were collected and de-chorionated using 50% commercial bleach for 3 mins. Following dechorionation, the embryos were washed with water on a nylon mesh, arranged on a piece of cut agar with the help of a fly stereomicroscope. The embryos were then desiccated using Silica gel in a desiccator for 10 minutes. The desiccated embryos were injected with either mitotic-anti-Sas-4 antibody (Sas-4-TT211p) or DMEM +10% FBS using an inverted microscope as described (Fish et al., 2007). The injected embryos were allowed to stand at RT for 30 mins. The embryos were then fixed and stained as described in the immunofluorescence and light microscopy section.

Immunofluorescence and light microscopy

For light microscopy, as well as for STED, the required amount of Schneider cells were seeded on concanavalin treated coverslips and allowed to adhere for 10 mins. The cells were then washed with PBS and fixed with 3.7% formaldehyde for 10 mins. Further, the cells were washed 2x times with PBS and permeabilized with 0.1% Triton X-100 in PBS (PBT) for 15 minutes, followed by blocking in PBT containing 2% Bovine serum albumin (BSA) for 30 mins.

Primary antibody staining was carried out at room temperature (RT) for 1 hr or overnight at 4°C. After labeling, the antibody was removed and the samples were washed 3x times with PBS. Further, the respective secondary antibodies along with DAPI were used against the primary antibody and incubated at RT for 1 hr. Confocal images were obtained using Olympus Fluoview FV1000 and Leica SP8 Laser scanning confocal microscope. For confocal microscopy, chromatic aberrations were checked using tetraspeck beads (Invitrogen).

STED imaging was performed using TCS SP8 gSTED, Leica. Far-red depletion laser (STED-Laser 775nm) was used for STED imaging. The alignment between channels was monitored using the Gatta STED Nanoruler (Gatta quant, Germany) to monitor STED performance. The PL Apo 100x/1.40 Oil STED Orange (Leica) objective was used, resulting in 100 × overall magnification with ~50nm lateral and 120nm axial resolution. Signals were detected using, gateable hybrid detectors (HyD). Nyquist sampling criteria was maintained during imaging to achieve *X-Y* resolution of 120nm. Images obtained were deconvoluted using Huygens essential deconvolution software. Line profiles were plotted based on fluorescent intensity values. The images were further processed using ImageJ and Adobe Photoshop.

For light microscopy of fly testes expressing the different Sas-4 variants, the dark pupae testes were dissected in PBS and transferred to a fixative solution containing 3.7% formaldehyde for 10 mins. The samples were then placed on pre-labeled slides and squished with the help of a coverslip and further immersed into liquid nitrogen for 30 s. The slides were removed and the coverslips were flicked off before placing them in a beaker, containing methanol for 10 mins. The samples were permeabilized with 0.1% Triton X-100 in PBS for 10 mins and blocked with 2% BSA, 0.1% Triton X-100 in PBS for 1 hr at RT. The samples were labeled with primary antibodies at RT for 1-2 hr or overnight at 4°C and further washed and labeled with secondary antibodies for 1 hr at RT along with DAPI. Analyses of the samples were carried out as described above. For the *Drosophila* neuroblast staining, the third instar larvae were dissected and stained similar to the testis staining.

Injected *Drosophila* embryos were transferred to a 1.5ml eppendorf containing the fixative (4% formaldehyde and 50% n-heptane in PBS) and incubated with constant rotation for 1 hr at RT. After fixation, 80% of the lower phase of the fixative was removed and the tube was filled with 1ml cold methanol and vortexed for 1 min. After most of the embryos settled to the bottom, the liquid was

removed, and the embryos were further washed thrice with methanol. PBT (PBS+0.3% Tritonx100) was used to re-hydrate the embryos followed by blocking using 2% BSA, 0.1% Triton X-100 in PBS for 1 hr at RT. Primary antibody staining was carried out overnight at 4°C. After labeling, the antibody was removed, and the samples were washed 3x times with PBT. The respective secondary antibodies along with DAPI were used against the primary antibody and incubated at RT for 4-5 hr. The embryos were washed 3x times with PBT and mounted on a slide containing two coverslips placed next to each other with a gap of 4 mm. The embryos were carefully placed in the gap and excess PBT was drained off. A third coverslip was then placed over the embryos with the help of Mowiol and allowed to dry. The embryos were imaged as described above.

Electron microscopy

Testes from *Drosophila* mid-aged pupae expressing different Sas-4 transgenes (Sas-4^{WT}, Sas-4^{TT211AA}, Sas-4^{SST198AAA} and Sas-4 $^{\Delta P1\text{-}P2}$) were dissected and transferred to a solution containing 2.5% glutaraldehyde buffered in PBS overnight at 4°C. The samples were washed with PBS and post-fixed in 1% osmium tetroxide in PBS for 2hrs at 4°C. Furthermore, the samples were carefully rinsed in PBS. The washed material was then dehydrated with graded series of ethanol; embedded in a mixture of Epon-Araldite resin and further polymerized for 48hrs at 60°C. Reichert Ultracut E ultramicrotome was used to obtain 60-70nm thick sections. The microtome consisted of copper grids with a mounted diamond knife, which was then stained with samarium triacetate and lead citrate. Morada CCD camera (Olympus) equipped Tecnai Spirit Transmission Electron Microscope (FEI) functioning at 100 kV was used to observe the samples. The images obtained were processed using Adobe Photoshop.(Fu et al., 2016)

Peptide generation and dot blot analysis

The peptides mentioned in Figure S1 were generated commercially (GenScript, NJ, USA). Peptides were thawed on ice prior to use. 5 micro-liters of each peptide (50 μM final conc.) were added to the nitrocellulose membrane and the membrane was allowed to dry for 15 minutes. The membrane was blocked using 5% milk in 1xTBST for 1 hr and then incubated with the primary antibodies overnight at 4°C. Next day the blots were washed with 1x TBST and then incubated with the respective secondary antibodies for 1 hr at RT. The membrane was further washed 3x times with 1x TBST and developed using the Super signal west pico/ femto chemilluminescent substrates that were used to detect the peroxidase activity in the samples.

In vitro kinase assay

The invitro kinase assay was as previously described (Novak et al., 2016). In brief, synthetic Sas-4 peptides (with a final concentration of 50 μM) were incubated with 200ng of Plk1/Polo, Cdk1 or AuroraA in 1x NEB buffer for protein kinases along with cold ATP (100 μM) for 30 mins at RT. For the inhibitor experiments, 1 μM BI2535 (Plk1/Polo inhibitor) was added to the reaction mixture containing Sas-4 peptide and Plk1/Polo kinase. The reaction was then stopped by adding 7.5M guanidine-hydrochloride. 2 μL from each of the mixtures were spotted onto nitrocellulose membranes for dot blot analysis as described above. The mitotic anti Sas-4 (Sas-4-TT211p) was used to analyze the phosphorylation status of peptides.

Antibody competition experiment

Mitotic anti-Sas-4 antibody (Sas-4-TT211p) and anti-Sas-4 antibody are treated with increasing concentrations of either non-phosphorylated Sas-4 peptide (207-YASSTTASSTSPRV-220, 0.9 μM and 3.5 μM) or Sas-4 phosphorylated peptide (207-YASS**TT**AS STSPRV-220, 0.9 μM and 3.5 μM). The antibodies are then used to label Sas-4 in Schneider cells as described in the immunofluorescence and light microscopy section.

Recombinant protein purification

Sas-4 1-350, Sas-4-TT211AA, Sas-4-SST198AAA and Sas-4 ΔP1-P2 were cloned in PGEX-6p and expressed in E-coli strain BL-21 (DE3) and the protein was induced using isopropylthiogalactoside. The cells were sonicated to release the proteins and spun at 25000 rpm to obtain lysate containing soluble fraction of the proteins. The proteins were purified using GST-agarose beads and then washed with buffer containing 50mM Tris-Hcl, 200mM Nacl (pH 8.0) and high salt buffer containing 50mM Tris-Hcl, 500mM Nacl (pH 8.0). The proteins are then cleaved overnight at 4°C using P3C precision enzyme. The supernatant was then concentrated and subjected to FPLC analysis. The fractions obtained were then tested by Coomassie staining as well as western blot for confirmation.

GST Pull-down assays

GST tagged recombinant proteins Sas-4 1-350, Sas-4-TT211AA, and Sas-4 ΔP1-P2 were expressed and purified as described above. The purified proteins bound to GST were incubated with *Drosophila* cell extracts lacking Sas-4 for 3 hours at 4°C. The beads were then washed with buffer containing 50mM Tris-Hcl, 200mM Nacl (pH 8.0) and high salt buffer containing 50mM Tris-Hcl, 500mM Nacl (pH 8.0) 3x times. The buffer was removed and the beads were boiled for 10 mins after adding 2x Laemmli buffer. The samples were then analyzed using western blotting.

For direct interaction analysis with Plk1/Polo, the GST tagged Sas-4 proteins bound to the beads were used as a bait to capture pure Plk1/Polo-GST protein from the supernatant. To clarify that the GST tag alone does not mediate the interaction between Sas-4 proteins and Plk1/Polo, recombinant GST protein was used as a negative control.

Immunoprecipitation (IP) of Sas-4 complexes

Protein G Sepharose beads (Sigma Aldrich) were coated with anti-Sas-4 antibody overnight at 4°C. The coated beads were then incubated with *Drosophila* embryonic high speed lysate (HSL) for 3hrs at 4°C. The lysates were prepared by lysing the embryonic extracts with 1x BRB80 buffer (extract buffer) as described by (Gopalakrishnan et al., 2011). After incubation, the beads were washed 1x times with extract buffer containing 1% triton x100 and 2x times with the extract buffer alone. The washed beads were then eluted by boiling them in 2x Laemmli buffer at 98°C. The beads were analyzed by western blotting for the Sas-4 complexes.

Western blotting and Coomassie staining

Protein samples in 4x Laemmli buffer were heated at 98°C for 10 mins before use. Samples were resolved using 10% polyacrylamide gels. The proteins were then transferred to nitrocellulose membrane for 1 hour at 135V. The membrane was blocked using 5% milk in 1xTBST for 1 hr and then incubated with the primary antibodies overnight at 4°C. Next day, the blots were washed with 1x TBST and then incubated with the respective secondary antibodies for 1 hr at RT. The membrane was further washed 3x times with 1x TBST and developed using the Super signal west pico/ femto chemilluminescent substrates that were used to detect the peroxidase activity in the samples.

For Coomassie staining, the samples were resolved in 12% polyacrylamide gel as described above. The gel was stained with Coomassie blue staining dye (10% methanol, 20% acetic acid, 70% water and 0.025% Coomassie dye) for 10 mins. De-staining was carried out using buffer containing 10% methanol, 20% acetic acid and 70% water.

QUANTIFICATION AND STATISTICAL ANALYSIS

Statistical analysis was carried out using Graph Pad Prism software (version 6.0). Student's T- test (Unpaired, one tailed) or ordinary one-way ANOVA followed by Tukey's multiple comparison tests were used to analyze the results. The error bars are expressed as mean ± s.e.m. Significance depicts p value (*$p < 0.05$, **0 < 0.001, ***$p < 0.0001$). The ''n'' represents number of centrosomes analyzed in interphase/ mitotic cells. The intensity of mitotic and interphase centrosomes were measured using ImageJ and were further calculated relative to controls.

Cell Reports, Volume *25*

Supplemental Information

Plk1/Polo Phosphorylates Sas-4 at the Onset of Mitosis for an Efficient Recruitment of Pericentriolar Material to Centrosomes

Anand Ramani, Aruljothi Mariappan, Marco Gottardo, Sunit Mandad, Henning Urlaub, Tomer Avidor-Reiss, Maria Riparbelli, Giuliano Callaini, Alain Debec, Regina Feederle, and Jay Gopalakrishnan

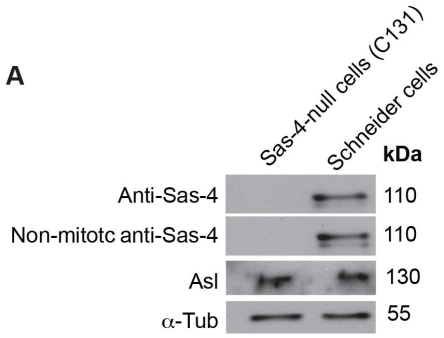
A
Sas-4-null cells (C131)
Schneider cells
kDa
Anti-Sas-4
110
Non-mitotc anti-Sas-4
110
Asl
130
α-Tub
55

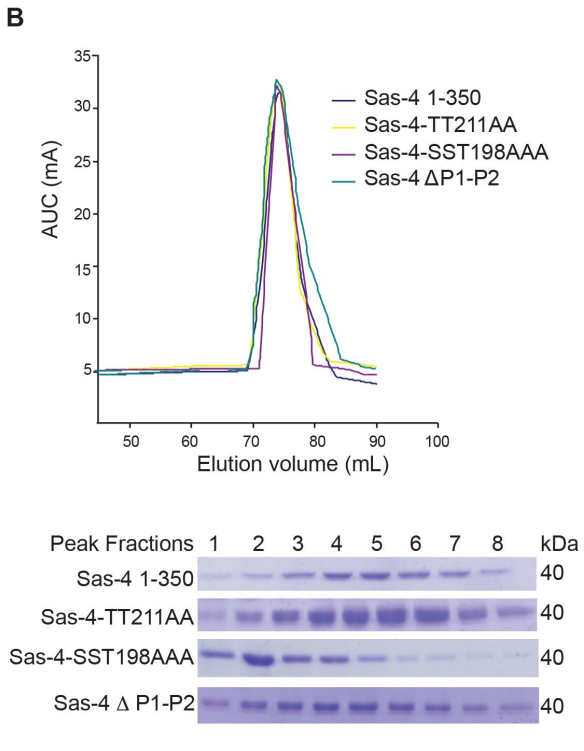
B
AUC (mA)
Elution volume (mL)
Sas-4 1-350
Sas-4-TT211AA
Sas-4-SST198AAA
Sas-4 ΔP1-P2
Peak Fractions 1 2 3 4 5 6 7 8
kDa
Sas-4 1-350
40
Sas-4-TT211AA
40
Sas-4-SST198AAA
40
Sas-4 Δ P1-P2
40

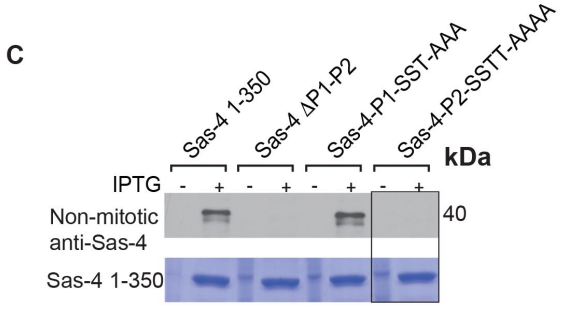
C
Sas-4 1-350
Sas-4 ΔP1-P2
Sas-4-P1-SST-AAA
Sas-4-P2-SSTT-AAAA
kDa
IPTG
Non-mitotic anti-Sas-4
40
Sas-4 1-350

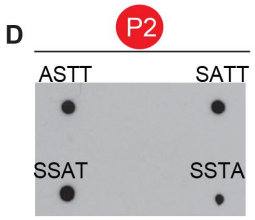
D
P2
ASTT
SATT
SSAT
SSTA

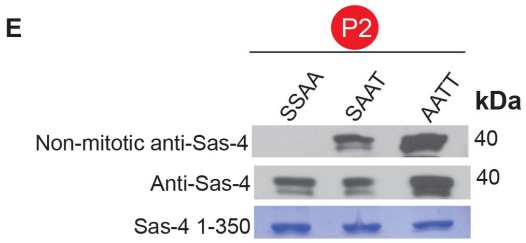
E
P2
SSAA
SAAT
AATT
kDa
Non-mitotic anti-Sas-4
40
Anti-Sas-4
40
Sas-4 1-350

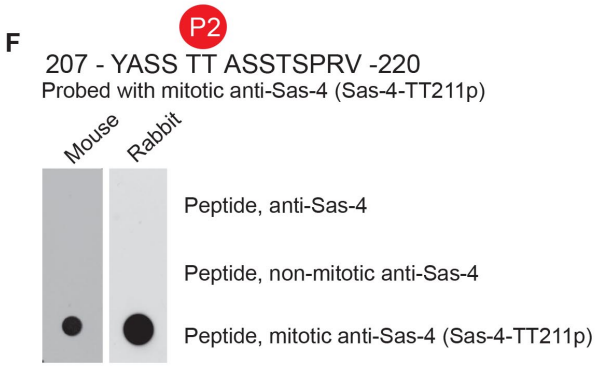
F
P2
207 - YASS TT ASSTSPRV -220
Probed with mitotic anti-Sas-4 (Sas-4-TT211p)
Mouse
Rabbit
Peptide, anti-Sas-4
Peptide, non-mitotic anti-Sas-4
Peptide, mitotic anti-Sas-4 (Sas-4-TT211p)

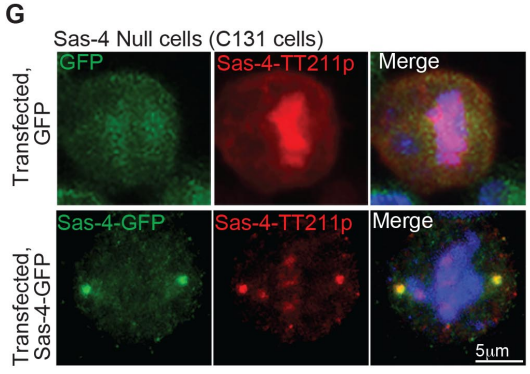
G
Sas-4 Null cells (C131 cells)
GFP
Sas-4-TT211p
Merge
Transfected, GFP
Sas-4-GFP
Sas-4-TT211p
Merge
Transfected, Sas-4-GFP
5μm

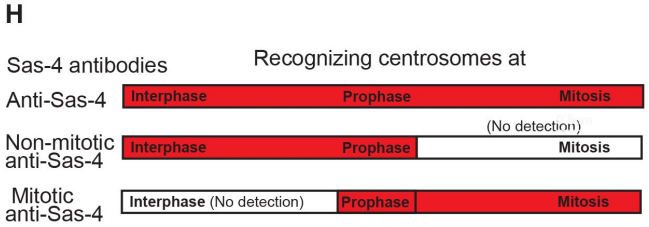
H
Sas-4 antibodies
Recognizing centrosomes at
Anti-Sas-4
Interphase
Prophase
Mitosis
Non-mitotic anti-Sas-4
(No detection)
Interphase
Prophase
Mitosis
Mitotic anti-Sas-4
Interphase (No detection)
Prophase
Mitosis

Figure S1. *In vitro* validation of anti-Sas-4, non-mitotic anti-Sas-4 and Sas-4-TT211p (mitotic specific Sas-4) antibody. Related to figures 1, 2 and 5.

(**A**) Western bot analysis to validate the Sas-4 antibodies using Schneider cells and Schneider cells lacking Sas-4 protein (C131 cells). The anti-Sas-4 antibody and the non-mitotic anti-Sas-4 antibody recognize Sas-4 only in the Schneider cells and not in the C131 cells. Tubulin and Asterless (Asl) are used as loading controls.
(**B**) Fast protein liquid chromatography (FPLC) analysis of purified Sas-4 1-350 variants. All of the variants elute at similar elution volume and have a similar area under the curve (AUC). Coomassie staining of peak fractions (fractions 1 to 8) is shown below.
(C) The non-mitotic anti-Sas-4 is specific for -P2 site. Coomassie blue staining of recombinant Sas-4 1-350 is given at the bottom panel. Plus sign (+) denotes IPTG induction of recombinant protein expression. Minus sign (-) denotes un-induced loading control.(**D**) Dot-blot shows that the non-mitotic anti-Sas-4 is able to recognize Sas-4 peptides (207-220aa) with single amino acid replacements at the -P2 site.
(**E**) The non-mitotic anti-Sas-4 is specific for Sas-4-TT211 as it fails to recognize double amino acid replacements at the -P2 site. Note in contrast to the non-mitotic anti-Sas-4, anti-Sas-4 recognizes all forms of the protein. Coomassie blue staining of recombinant Sas-4 1-350 is given at the bottom panel.
(**F**) Generation of mouse monoclonal and rabbit polyclonal anti-Sas-4 antibodies (Sas-4-TT211p) raised against phosphorylated peptide. This phosphorylated peptide (207-YASSpTpTASSTSPRV-220) is a specific substrate only for the mitotic anti-Sas-4 (Sas-4-TT211p).
(**G**) Schneider C131 cells (lacking Sas-4 protein) expressing –GFP (green, control) or Sas-4-GFP (green). The Sas-4-TT211p antibody (red) labels Sas-4 at mitotic centrosomes only in cells expressing Sas-4-GFP, showing that it is specific for Sas-4. Sas-4-TT211p seems to non-specifically label the DNA. Data not shown for Sas-4-TT211p raised in mouse.
(**H**) Schematic representation of the three different Sas-4 antibodies to compare the localization of Sas-4 at interphase and mitosis. The anti-Sas-4 antibody that recognizes centrosomal Sas-4 at interphase, prophase and metaphase (First bar). The non-mitotic anti-Sas-4 antibody recognizes Sas-4 only at the interphase and prophase (Middle bar); however, the mitotic anti-Sas-4 (Sas-4-TT211p) antibody recognizes Sas-4 only at pro-metaphase and metaphase of the cell cycle (Bottom bar).

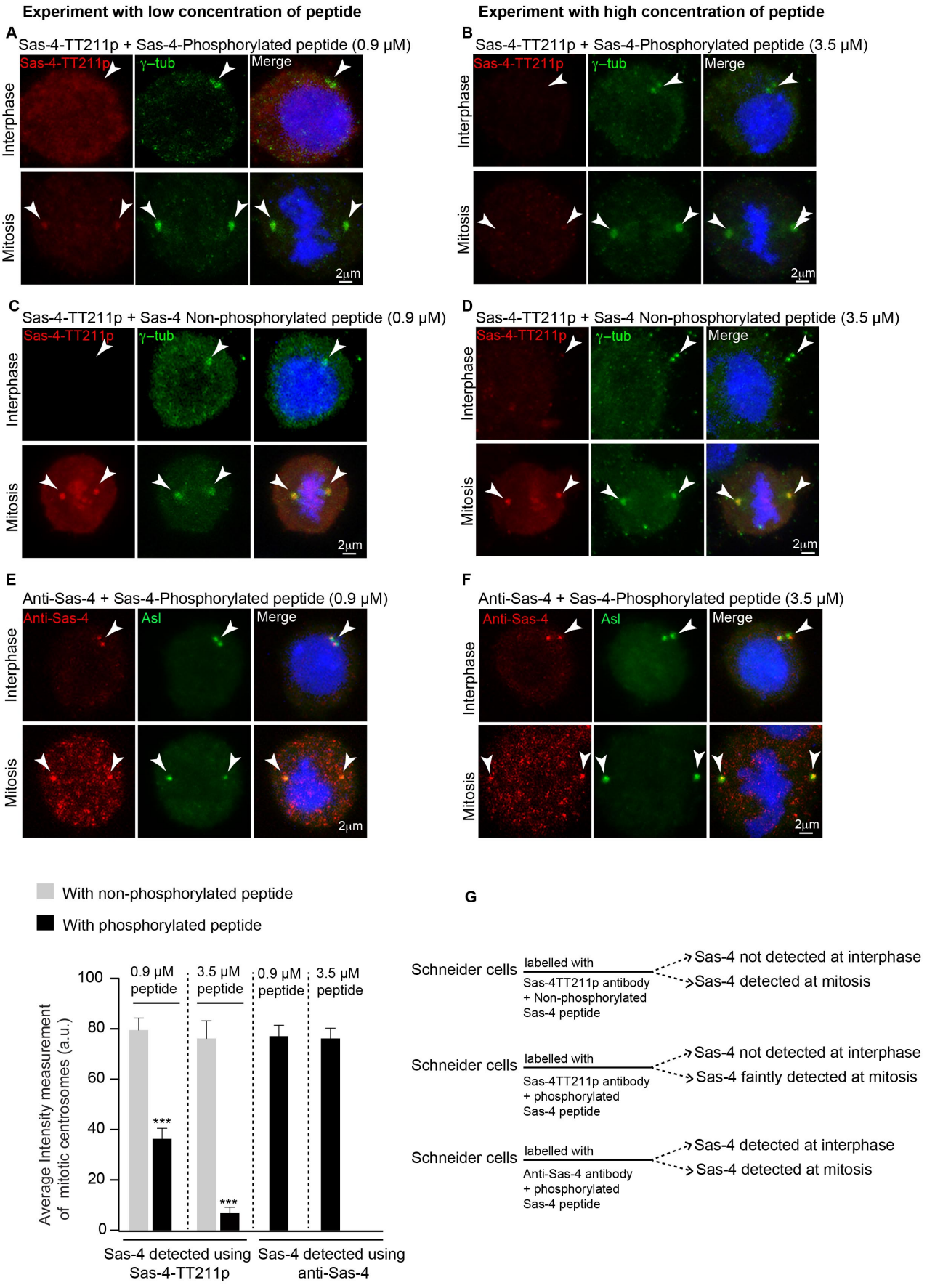

Figure S2. Sas-4 peptide-based competition experiment in Schneider cells. Related to Figures 2 and 5.

(**A-D**) Characterization of Sas-4-TT211p (red, mitotic-specific Sas-4 antibody) in the presence of increasing concentrations of Sas-4 phosphorylated peptide (207-YASS**TT**ASSTSPRV-220, 0.9 µM and 3.5 µM) or Sas-4 non-

phosphorylated peptide (207-YASSTTASSTSPRV-220, 0.9 μM and 3.5 μM). In the presence of higher concentration of Sas-4 phosphorylated peptide, Sas-4-TT211p failed to recognize mitotic Sas-4 (**A-B**). γ-tubulin (green) labels centrosomes. In contrast, Sas-4-TT211p normally labels Sas-4 at mitotic centrosomes in the presence of Sas-4 non-phosphorylated peptide (**C-D**). In either case, Sas-4-TT211p did not recognize Sas-4 at centrosomes of interphase cells. (**E-F**) Anti-Sas-4 antibody (red, whose epitope differs from Sas-4-TT211p) used as a control, recognizes Sas-4 at both interphase and mitosis in the presence of increasing concentrations of Sas-4 phosphorylated peptide. Asl (green) labels centrosomes. The arrowheads mark the centrosomes. The bar graph below represents the average intensity measurements of Sas-4 at mitotic centrosomes. At least 60 mitotic centrosomes *(n=60)* were analyzed from three independent experiments. ANOVA, ***$P<0.0001$. Error bars represent mean ± s.e.m.
(**G**) Experimental scheme of peptide-based competition experiment.

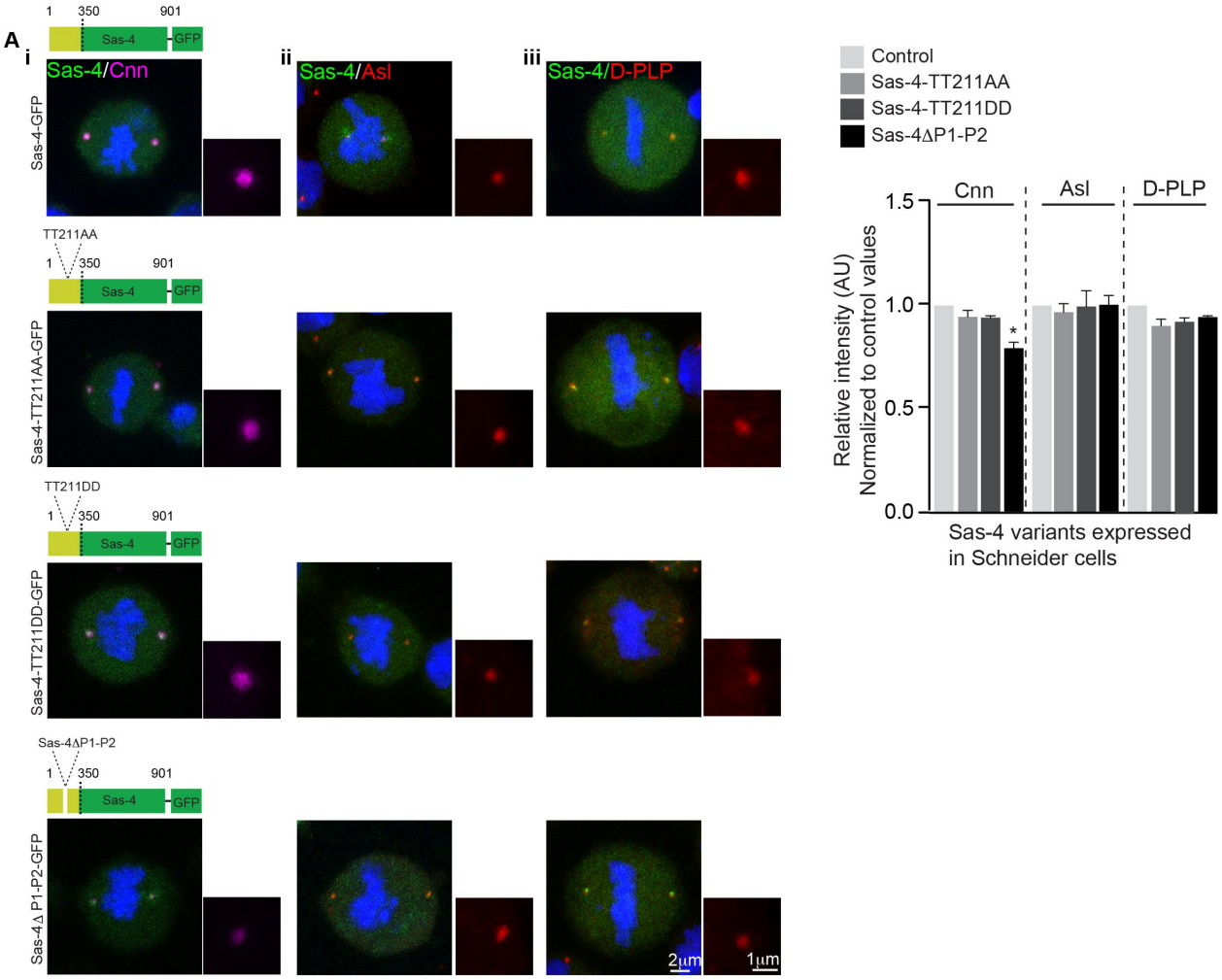

Figure S3. The Sas-4ΔP1-P2 mutation seems to mildly perturb the recruitment of Cnn to mitotic centrosomes in *Drosophila* Schneider cells. Related to figures 3 and 6.

(**A**) Schneider cells expressing different Sas-4 variants as -GFP (green). Sas-4ΔP1-P2 expressing cells showed mild defects in Cnn (**i**, magenta) recruitment at mitotic centrosomes. The bar graph on the right represents the relative intensity of PCM proteins at mitotic centrosomes. At least 40 mitotic centrosomes *(n=40)* were analyzed from three independent experiments. ANOVA, **P*<0.01. Error bars represent mean ± s.e.m.

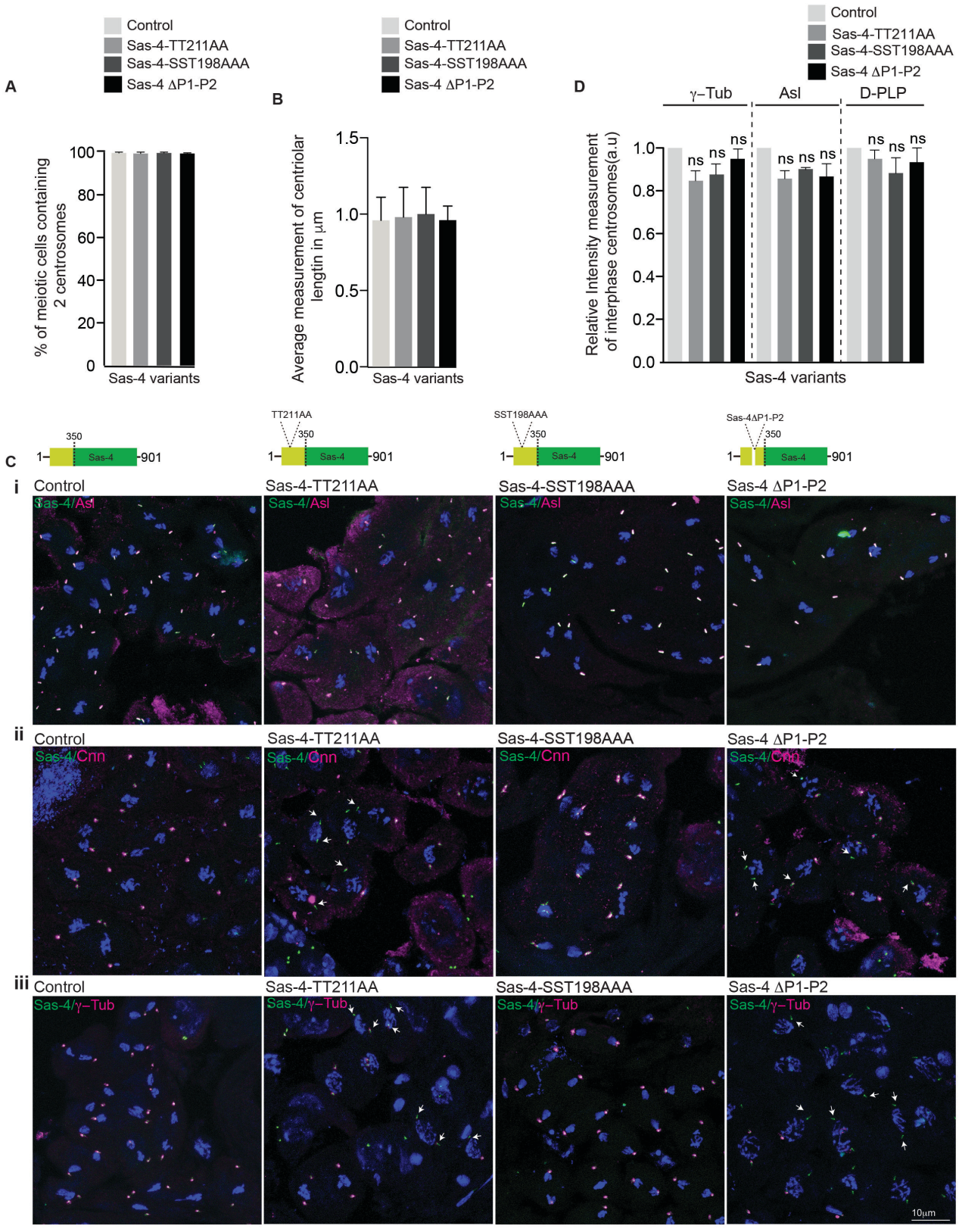

Figure S4. Sas-4 mutants used in this study do not alter centriolar numbers, lengths but perturb an efficient PCM recruitment. Related to figures 4 and 6.

(**A**) None of the Sas-4 variants display aberrant numbers of centrioles. At least 120 meiotic centrosomes (*n*=120) from testes were analyzed for each condition from three independent experiments. ANOVA. Error bars represent mean ± s.e.m.

(**B**) Flies expressing different Sas-4 variants show similar centriolar lengths. At least 80 meiotic centrosomes (*n*=80) from testes were analyzed for each condition from three independent experiments. ANOVA. Error bars represent mean ± s.e.m.

(**C**) Low magnification immunofluorescence images of meiotic cells of testes dissected from various Sas-4 variants. Note normal recruitment of Asl (magenta) in all of the Sas-4 variants **(i).** Defective recruitment of Cnn **(ii,** magenta**)** and γ-Tub **(iii,** magenta**)** is observed only in Sas-$4^{TT211AA}$ and Sas-$4^{\Delta P1\text{-}P2}$ transgenic flies.

(**D**) Bar graph representing the relative intensities of γ-tubulin, Asl and D-PLP at interphase centrosomes of mature spermatocytes expressing various Sas-4 variants. Note that these protein recruitments are not affected in any of the Sas-4 mutants. At least 60 meiotic centrosomes (*n*=60) from testes were analyzed for each condition from three independent experiments. ANOVA. Error bars represent mean ± s.e.m.

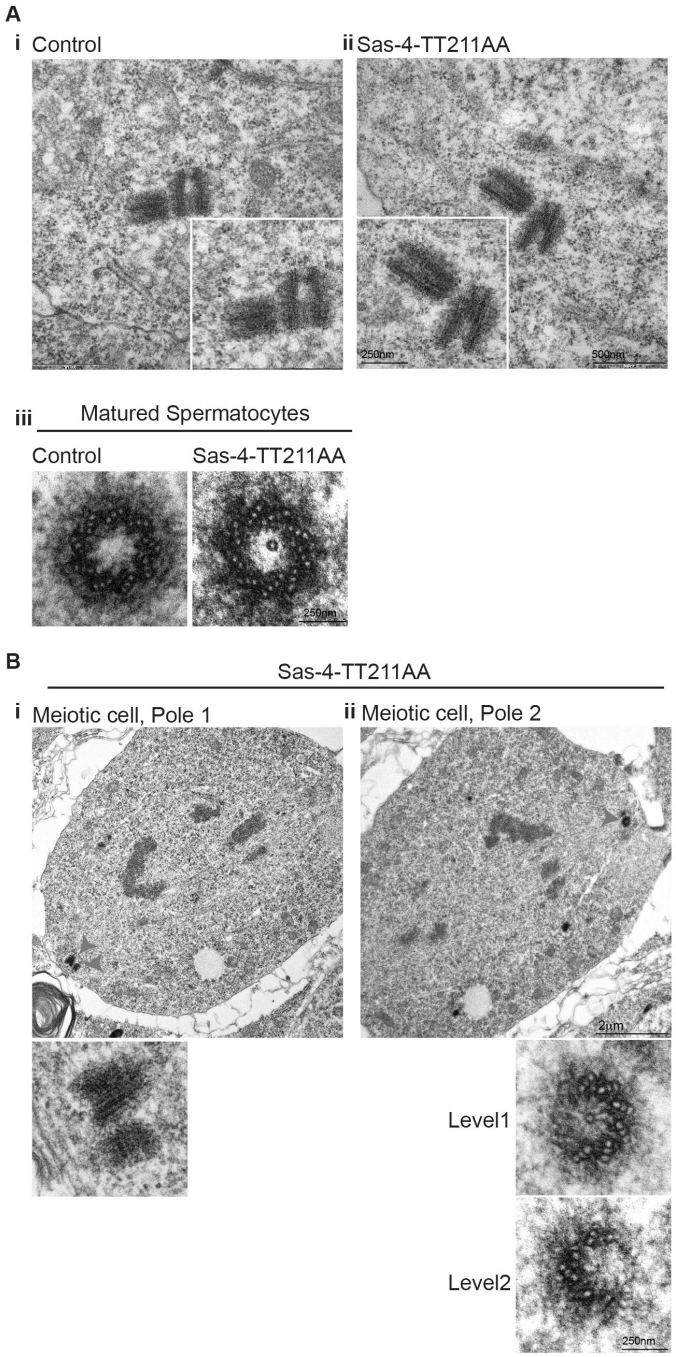

Figure S5. Sas-4^{TT211AA} expressing transgenic flies display structurally normal centrioles. Related to figures 4 and 6.

(**A**) EM micrographs showing normally looking centriole pairs in spermatocytes of control (Sas-4 wild type) **(i)** and Sas-4^{TT211AA} transgenic flies **(ii)**. Cross-sectioned centriolar structures of control (Sas-4 wild type) and Sas-4^{TT211AA} transgenic flies show no structural abnormalities **(iii).**

(B) Similarly, no defects are found in centrosomes of dividing spermatocytes of control (Sas-4 wild type) and Sas-4^{TT211AA} transgenic flies. Serial sectioning EM shows spindle poles (Arrowheads, **i** and **ii**) at two different slices. Cross sections show no defects in the over all structure of centrioles. Level 1 and level 2 are two adjacent sections. Note that the missing part of centriolar structure containing region of the level 1 is imaged at the level 2.

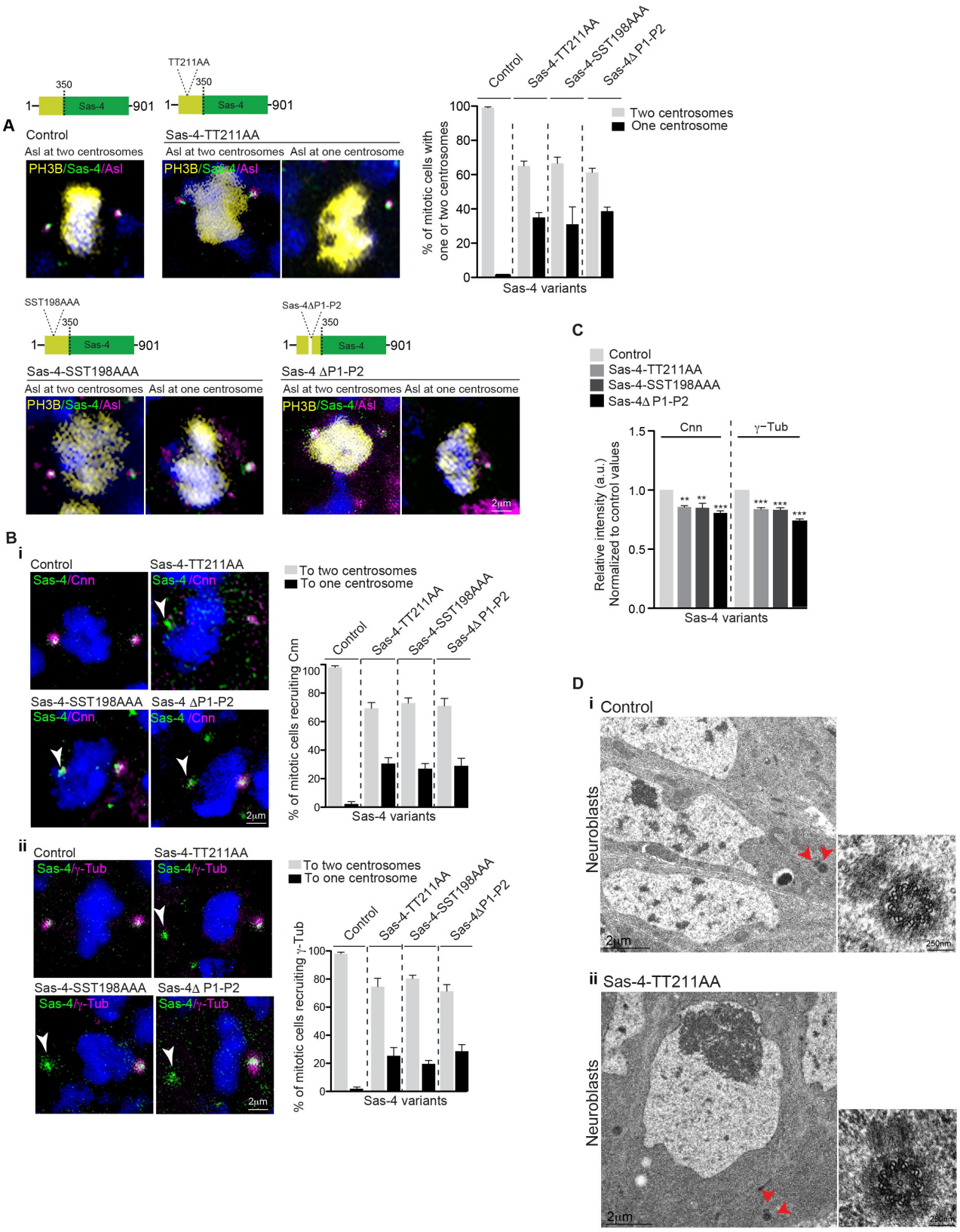

Figure S6. Sas-4-TT211 is required for an efficient recruitment of Cnn and γ-tubulin to the mitotic centrosomes of larval brain cells. Related to figures 6 and 7.

(**A**) Distribution of one and two-centrosome containing cells in various Sas-4 mutants as judged by the presence of Asl and Sas-4. Note Asl (magenta) recruitment appears to be unaffected. Anti-phospho-Histone H3 antibody (PH3B,

yellow) was used to identify mitotic cells. The bar graphs at right represent the percentage of mitotic cells recruiting Asl to either one or two centrosomes. At least 100 mitotic centrosomes (*n*=100) were analyzed for each condition from three independent experiments. ANOVA. Error bars represent mean ± s.e.m. Schematics representing the different Sas-4 mutations have been shown at the top for clarity.

(B) Reduced recruitment of Cnn (**i,** magenta) and γ-tubulin (**ii**, magenta) in two-centrosome containing mitotic cells expressing Sas-4^{TT211AA}, Sas-4^{SST198AAA} and Sas-4$^{\Delta P1\text{-}P2}$. The bar diagrams represent the percentage of mitotic cells recruiting Cnn and γ-tubulin to either one centrosome or both of the centrosomes. At least 80 mitotic centrosomes *(n=80)* were analyzed in each condition from three independent experiments. ANOVA. Error bars represent mean ± s.e.m.

(C) Bar graph representing the relative intensities of Cnn and γ-tubulin at mitotic centrosomes of larval neuroblasts expressing different Sas-4 mutations. Both Cnn and γ-tubulin recruitment is perturbed in flies expressing the different Sas-4 mutations. At least 80 mitotic centrosomes (*n*=80) from neuroblasts were analyzed for each condition from three independent experiments. ANOVA. ****P*<0.0001, ***P*<0.001. Error bars represent mean ± s.e.m.

(D) EM micrographs showing normally looking centriole pairs in interphase cells of larval neuroblasts of control (Sas-4 wild type) **(i)** and Sas-4^{TT211AA} transgenic flies, red arrow heads **(ii)**. Cross-sectioned centriolar structures of control (Sas-4 wild type) and Sas-4^{TT211AA} transgenic flies shows no structural abnormalities**.**